AEDC-TR-99-9

Implementation of a Virtual Camera for Ground Simulation of Store Separation Flight Test Film Data

K. S. Keen
Sverdrup Technology, Inc./AEDC Group

November 2000

Final Report for Period August 1997 through December 1998

Approved for public release; distribution is unlimited.

ARNOLD ENGINEERING DEVELOPMENT CENTER
ARNOLD AIR FORCE BASE, TENNESSEE
AIR FORCE MATERIEL COMMAND
UNITED STATES AIR FORCE

NOTICES

When U. S. Government drawings, specifications, or other data are used for any purpose other than a definitely related Government procurement operation, the Government thereby incurs no responsibility nor any obligation whatsoever, and the fact that the Government may have formulated, furnished, or in any way supplied the said drawings, specifications, or other data, is not to be regarded by implication or otherwise, or in any manner licensing the holder or any other person or corporation, or conveying any rights or permission to manufacture, use, or sell any patented invention that may in any way be related thereto.

Qualified users may obtain copies of this report from the Defense Technical Information Center.

References to named commercial products in this report are not to be considered in any sense as an endorsement of the product by the United States Air Force or the Government.

This report has been reviewed by the Office of Public Affairs (PA) and is releasable to the National Technical Information Service (NTIS). At NTIS, it will be available to the general public, including foreign nations.

APPROVAL STATEMENT

This report has been reviewed and approved.

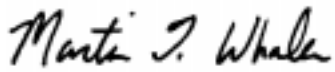

MARTIN T. WHALEN, Captain, USAF
Manager, Aircraft Systems Test Project
Aircraft Systems Test Division

Approved for publication:

FOR THE COMMANDER

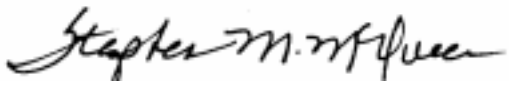

STEPHEN M. MCQUEEN, Lt Col, USAF
Chief, Aircraft Systems Test Division
Operations Directorate

REPORT DOCUMENTATION PAGE

Form Approved
OMB No. 0704-0188

The public reporting burden for this collection of information is estimated to average 1 hour per response, including the time for reviewing instructions, searching existing data sources, gathering and maintaining the data needed, and completing and reviewing the collection of information. Send comments regarding this burden estimate or any other aspect of this collection of information, including suggestions for reducing the burden, to Department of Defense, Washington Headquarters Services, Directorate for Information Operations and Reports (0704-0188), 1215 Jefferson Davis Highway, Suite 1204, Arlington, VA 22202-4302. Respondents should be aware that notwithstanding any other provision of law, no person shall be subject to any penalty for failing to comply with a collection of information if it does not display a currently valid OMB control number
PLEASE DO NOT RETURN YOUR FORM TO THE ABOVE ADDRESS.

1. REPORT DATE *(DD-MM-YYY)*	2. REPORT TYPE	3. DATES COVERED *(From - To)*
November 2000	Final Report	August 1997 - December 1998

4. TITLE AND SUBTITLE

Implementation of a Virtual Camera for Ground Simulation of Store Separation Flight Film Data

5a. CONTRACT NUMBER

5b. GRANT NUMBER

5c. PROGRAM ELEMENT NUMBER

6. AUTHOR(S)

K. S. Keen, Sverdrup Technology, Inc., AEDC Group

5d. PROJECT NUMBER

5e. TASK NUMBER

5f. WORK UNIT NUMBER

7. PERFORMING ORGANIZATION NAME(S) AND ADDRESS(ES)

Arnold Engineering Development Center/DOF
Air Force Materiel Command
Arnold Air Force Base, TN 37389-6000

8. PERFORMING ORGANIZATION REPORT NUMBER

AEDC-TR-99-9

9. SPONSORING/MONITORING AGENCY NAME(S) AND ADDRESS(ES)

Aeronautical Systems Center/YFT
Wright-Patterson Air Force Base, OH 45433-6503

10. SPONSOR/MONITOR'S ACRONYM(S)

11. SPONSOR/MONITOR'S REPORT NUMBER(S)

12. DISTRIBUTION/AVAILABILITY STATEMENT

Approved for public release, distribution is unlimited.

13. SUPPLEMENTARY NOTES

Available in Defense Technical Information Center (DTIC)

14. ABSTRACT

High-speed film recorded by cameras mounted on a flight test aircraft is one of the primary means of obtaining inflight data about the motions of fuel tanks, bombs, missiles, and other stores during separation. This reqport describes the development and implementation of computer graphics techniques to emulate the views of store release events expected to be obtained from flight test cameras positioned on the basis of pre-flight ground simulations. The computer visualization can be used to help place and o rient the cameras for optimum coverage of the expected store release motions.

15. SUBJECT TERMS

store separation, flight testing, ground testing, film data

16. SECURITY CLASSIFICATION OF:			17. LIMITATION OF ABSTRACT	18. NUMBER OF PAGES	19a. NAMES OF RESPONSIBLE PERSON
a. REPORT	b. ABSTRACT	c. THIS PAGE			Stephen M. McQueen, Lt Col, USAF
Unclassified	Unclassified	Unclassified	U	48	19b. TELEPHONE NUMER *(Include area code)* 931-454-7369

PREFACE

The work reported herein was conducted at the Arnold Engineering Development Center (AEDC), Air Force Materiel Command (AFMC). The major portion of the development effort was sponsored by the store separation effort for the F-22 aircraft at the request of the Aeronautical Systems Center (ASC/YFT) under AEDC Project Number 0675. The ASC/YFT Project Manager was Mr. Pete Amstutz. The results were obtained by Sverdrup Technology Inc., a Jacobs Engineering Company, support contractor for testing at AEDC, AFMC, Arnold Air Force Base, TN. The work was conducted during the period August 1997 through December 1998, and the manuscript was submitted for publication on September 13, 2000.

The author would like to acknowledge the work of colleagues Ric Clippard and Mary Craig, developers of the current version of the AEDC store-separation graphics analysis code, and Mark Smith, designer of an early prototype camera-modeling capability.

CONTENTS

ILLUSTRATIONS

TABLES

1.0 INTRODUCTION

Film data recorded at onboard camera stations on a flight test aircraft are one of the primary information sources for certifying safe and acceptable flight releases of tanks, bombs, missiles, and other stores from the aircraft. This report describes the development and implementation of a capability to use computer graphics techniques to emulate the views which are obtained from flight test cameras on the basis of pre-flight ground simulations of the store motions generated in wind tunnel tests. The computer graphics visualizations can be used to help place and orient the flight test cameras for maximum coverage of the expected store motions and can also be used for pre-flight checkout of the flight data-reduction procedures. The camera views can also be used to greatly speed up flight- and ground-test data comparisons. If computer views of the ground simulation match the flight film, then the time-consuming and laborious process of reading the flight film and reducing trajectory data from it can be performed in a less intensive fashion. Decisions about whether to proceed to the next flight test point can then be made before the reduced flight film data become available.

The graphics techniques were developed during efforts to support wind tunnel testing of the F-22 aircraft, and most of the applications to this point have been directed toward that aircraft. Although the techniques are applicable to any aircraft, it was thought that the readability of the current presentation would be enhanced if applications to the specific F-22 case were described. The purpose of the report, however, is to describe the computer graphics techniques themselves and not, in any way, to analyze F-22 separation performance.

The camera-modeling techniques have been implemented within the framework of the existing AEDC computer-graphics trajectory analysis code. The basic store separation computer graphics capabilities are described in Ref. 1. Since the publication of Ref. 1, a more modern implementation of the basic store separation graphics capability has been accomplished, and the code has been renamed the Trajectory VISualization (TVIS) program.

2.0 A COMPUTER GRAPHICS CAMERA MODEL

The mathematical modeling of the flight camera graphics views is described in this section. The actual camera systems are described in Section 2.1. The mathematical modeling of the cameras is described in Section 2.2. The three-dimensional (3-D) mathematical implementation of the graphics views is then described in Section 2.3.

2.1 DESCRIPTION OF FLIGHT TEST CAMERA EQUIPMENT

The cameras to be used on the F-22 are Photo-Sonics Inc. model 1VN standard 16-mm film cameras. The same make and model cameras have been used on previous flight test programs on other aircraft, such as the F-15 and F-16, at Eglin and Edwards Air Force Bases. Information specification (spec) sheets on the 1VN cameras were obtained from two sites on the World Wide Web - www.photo-sonics.com and www.photosonics.com. The cameras are lightweight (camera

body weight of only 1.5 lb) and compact, and they are equipped with automatic exposure control for changing light levels. They are ideally suited for flight test applications. The cameras operate at a speed of 200 frames per second, which results in a flight test trajectory data time step of 0.005 sec. Film magazines containing 100 ft of 4-mil film allow for a maximum of 20 seconds of data per camera. (Usually a delay is built into the store release sequence so that the cameras are allowed to run for several seconds before release.) Each camera also has an associated Photo-Sonics Inc. Film Data Recording System (FDRS) module. The modules are used to optically encode IRIG-B time information (and perhaps other information) on one side of the main film frame area. The time information may be used to synchronize the film from the different cameras. The camera is deliberately designed to expose a larger area on the film frame than do most standard 16-mm cameras. This is accomplished by using a circular window truncated at the top and bottom of the film frame. The aperture size of the 1VN camera is quoted in a spec sheet from the Web site as 0.552 in. wide (maximum) × 0.296 in. high (14.0208 mm × 7.5184 mm) with a height/width aspect ratio of 0.53623. "Standard" 16-mm film frames are nominally 0.410 in. × 0.292 in. (10.414 mm × 7.41 mm), corresponding to an aspect ratio of 0.71219. A typical frame of 16-mm film showing the 1VN and standard aperture sizes is presented in Fig 1. Special film projectors are required to display the full 1VN film frame because of its nonstandard (larger) frame size.

Most of the information herein about camera locations on the F-22 flight test aircraft was extracted from preliminary F-22 Flight Test Request (FTR) Number 60045, Revision 0 and preliminary Test Information Summary (TIS) AR020. At the time the virtual camera models were first implemented, the first F-22 store separation flight tests were still some years in the future, and much of the information from those documents was still preliminary or to-be-determined. As flight test planning efforts have advanced, some F-22 camera information has been updated, but that information is not germane to the present documentation of the graphic camera techniques. Eleven primary camera stations (Station 8 has been deleted) are being designed for the F-22 flight test aircraft as shown in Fig 2. Camera number 5 is inside a universal pod mounted to the lower surface of the aircraft fuselage and can be set to arbitrary camera yaw line-of-sight angles ranging from the 1 o'clock position (looking forward and slightly to the right) through the 9 o'clock position (looking full left) to the 5 o'clock position (looking aft and slightly to the right). Camera 5 can also be set to pitch angles of 0, 10, 20, or 30 deg below the aircraft horizontal plane. The other cameras are bolted in place on special brackets and provide fixed views. Three cameras are proposed to be mounted within the aircraft wing pylons. Positioning of the pylon cameras was still to be determined at the time of the first implementation of the virtual camera model because the pylon design was not then finalized. Camera station 4 is inside the left flare/chaff countermeasures bay. The door of the bay on the flight test aircraft will be fitted with a glass window to allow visual access for this camera. Camera station 12 is inside the side weapons bay and is intended to provide a close-up view of the clearance between the front edge of the side bay doors and the AIM-9M missile tails. Various hole patterns are available in the mounting brackets for some of the fixed cameras so that they may be aimed to provide maximum coverage for certain anticipated store motions. Figure 3, for example, shows the four available mountings for the camera at station 4. Figure 4 shows the line-of-sight directions for the four possible mountings

of Camera 4 with an indication of the camera field of view for each mounting. The four different mountings have been designated stations 4a through 4d. Table 1 (reproduced from the first edition of TIS AR020) lists the absolute aircraft coordinates (fuselage station, buttock line, waterline) of each camera station.

Two different lenses will be used on the 1VN cameras in F-22 store separation flights. One is a straight Angenieux model R7 5.9-mm focal length f/1.8 lens (Photo-Sonics part number 95014). The other lens is described as a "right-angle" lens with a focal length of 10.0 mm. Its make and model were not specified in either FTR 60045 or TIS AR020. The 5.9-mm lens produces a field of view quoted in TIS AR020 as 70 deg vertical × 90 deg horizontal. The 10-mm lens provides a quoted 41- × 55-deg field of view. A spec sheet provided by Photo-Sonics quotes the Angenieux 5.9-mm lens field of view as 94 deg as shown in Fig. 5. Further discussions of field of view are provided in Section 2.2. Note the front nodal point for the Angenieux lens which is called out in Fig. 5. The front nodal point approximates the idealized viewpoint of the lens and will be used as such in the implementation of the virtual camera model. This point will be assumed to be the point of perspective convergence for the computer-graphics views. Referring to Fig. 3, note that the camera mounting brackets were designed so that this point on the lens would be at approximately the same aircraft coordinates for all camera angles. Referring again to Table 1, note that one of the columns is labeled the "Location"; it is assumed herein that these coordinates refer to the front nodal point of the lenses (since the aircraft coordinates of the point where the lenses attach to the cameras are different for every camera angle).

For any given flight separation, only certain cameras and certain camera orientations will be used, depending on the expected motion of the store. The cameras to be used for each flight are specified in a camera "setup" table. Setup A, for example, might list all the cameras and mounting positions that should get a good view of AIM-9M rail launches from the F-22 side bay. Before the flight, ground personnel would be responsible for ensuring that all of the specified cameras were loaded with film, that each fixed camera was mounted at the bracket hole positions specified in setup A, and that the universal camera (Camera no. 5) was rotated to the angles specified for setup A.

2.2 OVERVIEW OF GEOMETRICAL OPTICS USED IN THE VIRTUAL CAMERA MODEL

The subject of geometric lens optics is covered on an elementary level in any number of standard texts on the subject. The author has found, however, that detailed information for complex multi-element lenses which may be needed for more exact implementation of a virtual camera model is often lacking. For this reason some assumptions were necessary in the camera modeling presented in this section.

Before the approximations involved in modeling realistic multielement lens/camera systems are discussed, the idealized "simple" one-element camera will be described, as this idealized case

is more compatible with the limitations of many modern computer graphics programming techniques. The simple camera consists of a single lens element, an aperture, and a film plane. The most important physical property of the simple, one-element lens is its focal length, f. The focal length is the distance from the lens at which parallel light rays passing through the lens are focused to a point. The focal length is illustrated in Fig. 6. If the object that the simple one-element camera is looking at is at an infinite distance from the camera, then the rays of light from a point on the object which pass through the lens may be considered to be essentially parallel (or "paraxial") and to intersect at the "focal plane." The focal plane is where the film would be located for a "simple" camera focused at infinity. The "field of view" for the simple, one-element lens/camera focused at infinity is a simple geometric quantity dependent on the focal length and the dimensions of the film frame as shown in Fig. 7. In particular, the vertical field-of-view angle, FOVy, is given by:

$$\mathrm{FOVy} = 2 * \mathrm{Tan}^{-1}\left(\frac{\mathrm{film\_frame\_height}/2}{\mathrm{f}}\right) \tag{1}$$

and the horizontal field of view is given by:

$$\mathrm{FOVx} = 2 * \mathrm{Tan}^{-1}\left(\frac{\mathrm{film\_frame\_width}/2}{\mathrm{f}}\right) \tag{2}$$

If the simple thin lens is observing an object that is not at an infinite distance from the lens, then the image distance is related to the object distance by the Gaussian lens formula:

$$\frac{1}{\mathrm{o}} + \frac{1}{\mathrm{i}} = \frac{1}{\mathrm{f}} \tag{3}$$

The image distance is equal to f when the object is at infinity (1/o = 0.0 in Eq. [3]), but i is greater than f when the focus is on an object at a finite distance from the lens, as shown in Fig. 8. "Focusing" for a simple camera may be accomplished by a screw mechanism that moves the lens forward as it is rotated, thereby increasing the image distance, i, between the lens and the film plane. Inspection of Fig. 8 reveals that the field of view is somewhat reduced when the image distance is increased (the distance i replaces the distance f in Eqs. [1] and [2]).

When a real camera lens is focused on an object at any distance in front of the camera, there is an additional region in front of and behind the object that is also in focus. This in-focus region is called the "depth of field" and is a function primarily of the aperture or light-receiving area of the lens. For the F-22 camera models, the assumption was made that all cameras are focused at infinity. This assumption may be supported by the description of the Angenieux lens in the spec sheet of Fig. 5. The spec sheet discloses that this is a fixed-focus lens and that its depth of field

extends from 20 in. in front of the camera to infinity. This assumption may be an item of concern for the camera at station 12 in the side bay, as this camera is designed to image door-to-fin clearances in the near field. The station 12 camera may need to be focused for a near object rather than an infinitely distant object to get the door/missile within its depth of field.

Graphical camera modeling becomes more complicated when the simple, idealized lens is replaced with a realistic, multielement lens. At this point the information available in standard texts also becomes more nebulous, and some simplifying assumptions were necessary for the graphical models. A system of lenses in combination such as the Angenieux R7 may be replaced with an "equivalent" simple thin lens which has an equivalent focal length (5.9 mm for the R7). This equivalent focal length is usually determined experimentally by the lens manufacturer and is published in the lens spec (Fig. 5). Other equivalent properties of the composite lens may also be determined experimentally. One such property is the quoted field-of-view angle (94 deg) published in the R7 spec. Another measure that can be related to the lens field of view is the "exit pupil", which is called out in Fig. 5.

The real camera systems were simplified for the graphics views by modeling the actual multi-element camera/lens systems as 5.9- or 10-mm focal length "simple" cameras focused at infinity according to the simple model previously shown in Fig. 7. Using the expanded film frame of the 1VN camera (0.296 by 0.552 in.) and Eqs. (1) and (2), the field-of-view angles for the equivalent 5.9-mm camera are computed to be FOVx = 99.8316 deg and FOVy = 65.0067 deg. No attempt was made to model the circular left and right sides of the 1VN film frame or the missing corners of the frame caused by the film sprocket holes (Fig. 1). Instead, a rectangular area encompassing the actual frame was modeled. These computed 1VN frame values compare with horizontal and vertical field-of-view values of 90 and 70 deg, which are quoted in F-22 TIS AR020, and the single value of 94 deg specified in Fig 5. For the "simple" 10-mm camera the computed field-of-view angles are FOVx = 70.0639 deg and FOVy = 41.2045 deg, which do not compare as well with values of FOVx = 55 deg and FOVy = 41 deg quoted in TIS AR020. If a standard film frame is assumed (0.410 by 0.292 in.), then the 5.9-mm camera values are FOVx = 82.8595 deg and FOVy = 64.258 deg, and the 10-mm values are FOVx = 55.0119 deg and FOVy = 40.6593 deg. The 1VN field-of-view numbers computed from simple-camera equations (Eqs. [1] and [2]) are used in the virtual camera model.

2.3 MATHEMATICAL MODELING OF THE CAMERA AND AIRCRAFT FOR COMPUTER VISUALIZATION

2.3.1 Basics of Computer Graphics Mathematics

Each 3-D body making up a computer-graphic "scene" is modeled numerically as an ordered system of points, p, which are defined relative to some geometry axis system which has been specified for that body. For illustrative purposes, a case involving a missile attached to a rail which is, in turn, attached to an adaptor, which is attached to a pylon, which is attached to a wing,

which is, finally, attached to the aircraft is considered. The selected case is representative of the complexity involved in visualizing F-22 missile cluster trajectories. Each one of the geometry items has an associated axis system, which for the following equation derivations is designated by a single letter as shown in Fig 9. The "G" axis system is the basic system for the Global aircraft geometry. "W" denotes the Wing geometry system, "P" denotes the Pylon system, "A" denotes the Adaptor system, "R" denotes the Rail system, and, finally, "M" denotes the Missile system. The various 3-D graphical geometries involved in a store-separation "scene" are placed in the numerical configuration by specifying the position and orientation of the local geometry axis system of each piece relative to the local geometry axis system of the piece to which it is attached. Eventually, a system of referenced geometry transformations is created such that each locally defined geometry point may be redefined relative to the global geometry axis system of the entire aircraft, "G." At this point, the entire graphics "configuration" is assembled. The final step in virtual-camera graphic visualization is to position and orient this combined geometry relative to a camera axis system, which is denoted by "C."

Assembly of the graphics transformations can be explained from two opposite perspectives. According to the first philosophy, the relative positioning of the parts can be specified by defining a mathematical transformation matrix which describes the position and orientation of the axis system in which the "child" part is defined relative to the axis system of the "parent" part. According to the second philosophy, a different mathematical transformation matrix is developed which directly converts child-geometry-axis coordinates into parent-geometry-axis coordinates. It turns out (as is demonstrated) that the transformation matrix developed from the first philosophy is the mathematical transpose of the transformation developed from the second philosophy. The first philosophy is selected for the following derivation because it is analogous to the methods used in AEDC motion simulations (Ref. 2). After the mathematical derivation is presented, some comments are offered concerning how the transformations are implemented in OpenGL®, a modern graphics language which generally approaches geometry transformations from the second philosophy.

Each geometry component is located in the configuration by specifying the position and orientation of its axis system relative to the axis system of the piece to which it is attached. For example, the pylon is positioned translationally relative to the wing by specifying the Wing-axis components of the position vector of the Pylon-axis origin, P, relative to the Wing-axis origin, W. This position vector is written as {XWPW, YWPW, ZWPW} using a special nomenclature in which the second character of each name denotes the system in whose component directions the vector is measured (in this case, Wing-axis components), the third character represents the point of interest (the origin of the Pylon system), and the last character represents the point relative to which the distance is defined (the origin of the Wing system). Similarly, the pylon is positioned rotationally relative to the wing by specifying a 3×3 direction cosine matrix (Section 4.2.3.2 of Ref. 2) to define the orientation of the three Pylon-axis coordinate directions (X_P, Y_P, and Z_P) relative to the Wing-axis coordinate directions (X_W, Y_W, and Z_W). This matrix is written as [TRNPW] in the special nomenclature. The terms of the [TRNPW] direction-cosine matrix are

often obtained from yaw-pitch-roll sequence modified Euler angles, PSIPW, THAPW, PHIPW, according to the relations of Eq. 1.3.8 of Ref. 2. The {XWPW} vector and the [TRNPW] matrix describe the position and orientation of the Pylon axis system relative to the Wing axis system as described in the first philosophy.

The object of the remaining mathematical derivation is to develop the transformations needed to convert geometry points from one system to another so that, ultimately, all individual geometry coordinates can be transformed to the camera viewing system. Using the relationship between the wing and pylon geometry systems as an example, note that the [TRNPW] matrix can be used to project vector components measured in the Wing-axis directions to components defined in the Pylon-axis directions. For example, if vector {XWpW} represents the Wing-axis components of the position of arbitrary point p, relative to point W, then the vector {XPpW} given by:

$$\begin{vmatrix} XPpW \\ YPpW \\ ZPpW \end{vmatrix} = [TRNPW] \begin{vmatrix} XWpW \\ YWpW \\ ZWpW \end{vmatrix} \tag{4}$$

defines the Pylon-axis components of that same point relative to point W. This actually is not a particularly useful rotation, however, because it is more commonly necessary to convert points in the lower level system (in this case, the Pylon system) to the higher level system. The inverse of the [TRNPW] matrix, which is denoted by [TRNWP] = $[TRNPW]^{-1}$, can be used to perform this transformation:

$$\begin{vmatrix} XWpP \\ YWpP \\ ZWpP \end{vmatrix} = [TRNWP] \begin{vmatrix} XPpP \\ YPpP \\ ZPpP \end{vmatrix} = [TRNPW]^{-1} \begin{vmatrix} XPpP \\ YPpP \\ ZPpP \end{vmatrix} \tag{5}$$

One of the properties of a 3×3 direction cosine matrix is that its inverse is identical to its transpose; thus, [TRNWP] = $[TRNPW]^{-1}$ = $[TRNPW]^{T}$. This matrix property holds only for a special class of so-called “orthogonal” transformations, which includes rotational transformations. Using this property, which is proved in Section 4.2.3.2 of Ref. 2, a Pylon-axis geometry point such as {XPpP} can be projected to Wing-axis components by:

$$\begin{vmatrix} XWpP \\ YWpP \\ ZWpP \end{vmatrix} = [TRNWP] \begin{vmatrix} XPpP \\ YPpP \\ ZPpP \end{vmatrix} = [TRNPW]^{T} \begin{vmatrix} XPpP \\ YPpP \\ ZPpP \end{vmatrix} \tag{6}$$

Combining the rotational transformation from Eq. (6) with the origin-translation vector, we see that the Pylon-axis components of the position of point p relative to the Pylon-axis system can be transformed into Wing-axis components of the position of point p relative to the Wing-axis system according to:

$$\begin{vmatrix} XWpW \\ YWpW \\ ZWpW \end{vmatrix} = [TRNPW]^T \begin{vmatrix} XPpP \\ YPpP \\ ZPpP \end{vmatrix} + \begin{vmatrix} XWPW \\ YWPW \\ ZWPW \end{vmatrix} \tag{7}$$

Equation (7) is the fundamental relation used to transform points defined in individual local geometry axes to the axis system of the geometry to which it is attached. Repeated application of equations of the form of Eq. (7) can be used for multiple levels of referencing. For example, suppose that point p was originally a geometry point for the adaptor. An equation exactly analogous to Eq. (7) can be written for transforming that point to the pylon system:

$$\begin{vmatrix} XPpP \\ YPpP \\ ZPpP \end{vmatrix} = [TRNAP]^T \begin{vmatrix} XApA \\ YApA \\ ZApA \end{vmatrix} + \begin{vmatrix} XPAP \\ YPAP \\ ZPAP \end{vmatrix} \tag{8}$$

Substituting Eq. (8) into Eq. (7) then allows that Pylon-system point to be converted to the Wing-axis system:

$$\begin{vmatrix} XWpW \\ YWpW \\ ZWpW \end{vmatrix} = [TRNPW]^T \left([TRNAP]^T \begin{vmatrix} XApA \\ YApA \\ ZApA \end{vmatrix} + \begin{vmatrix} XPAP \\ YPAP \\ ZPAP \end{vmatrix} \right) + \begin{vmatrix} XWPW \\ YWPW \\ ZWPW \end{vmatrix} \tag{9}$$

It can be seen that multiple levels of referencing (for example, geometry points in the Missile system being transformed to the Rail system, then to the Adaptor system, then to the Pylon system, then to the Wing system, and finally to the Global system) would result in an extremely complicated expanded form of Eq. (9). Fortunately, a shorthand augmented matrix form of the transformation process is available which greatly simplifies the math. The augmented matrix involves a 4×4 partitioned matrix combining translation and rotation according to:

$$[\text{TMXPW}] = \begin{bmatrix} \text{TMXPW}(1,1) & \text{TMXPW}(1,2) & \text{TMXPW}(1,3) & \text{TMXPW}(1,4) \\ \text{TMXPW}(2,1) & \text{TMXPW}(2,2) & \text{TMXPW}(2,3) & \text{TMXPW}(2,4) \\ \text{TMXPW}(3,1) & \text{TMXPW}(3,2) & \text{TMXPW}(3,3) & \text{TMXPW}(3,4) \\ \text{TMXPW}(4,1) & \text{TMXPW}(4,2) & \text{TMXPW}(4,3) & \text{TMXPW}(4,4) \end{bmatrix}$$

$$= \begin{bmatrix} & & & 0 \\ & [\text{TRNPW}] & & 0 \\ & & & 0 \\ \text{XWPW} & \text{YWPW} & \text{ZWPW} & 1 \end{bmatrix} \qquad (10)$$

$$= \begin{bmatrix} \text{TRNPW}(1,1) & \text{TRNPW}(1,2) & \text{TRNPW}(1,3) & 0 \\ \text{TRNPW}(2,1) & \text{TRNPW}(2,2) & \text{TRNPW}(2,3) & 0 \\ \text{TRNPW}(3,1) & \text{TRNPW}(3,2) & \text{TRNPW}(3,3) & 0 \\ \text{XWPW} & \text{YWPW} & \text{ZWPW} & 1 \end{bmatrix}$$

This matrix form should not be interpreted as indicating that translation/rotation is a four-dimensional (4-D) process; it should, instead, be interpreted as indicating that the two 3-D processes of translation and rotation can be represented in one 4×4 partitioned matrix. The terms in the rightmost column of the augmented matrix can be related to perspective, shearing, and scaling transformations. These terms will never be changed from the values shown in Eq. (10) because most modern graphics languages implement perspective transformations most efficiently with a separate "viewing" matrix and accelerated graphics software/hardware.

Using the Eq. (10) form, we can rewrite Eq. (7) as:

$$\begin{vmatrix} \text{XWpW} \\ \text{YWpW} \\ \text{ZWpW} \end{vmatrix} = \begin{bmatrix} \text{TMXPW}(1,1) & \text{TMXPW}(2,1) & \text{TMXPW}(3,1) \\ \text{TMXPW}(1,2) & \text{TMXPW}(2,2) & \text{TMXPW}(3,2) \\ \text{TMXPW}(1,3) & \text{TMXPW}(2,3) & \text{TMXPW}(3,3) \end{bmatrix} \begin{vmatrix} \text{XPpP} \\ \text{YPpP} \\ \text{ZPpP} \end{vmatrix} + \begin{vmatrix} \text{TMXPW}(4,1) \\ \text{TMXPW}(4,2) \\ \text{TMXPW}(4,3) \end{vmatrix} \qquad (11)$$

where the row and column indices of the rotational part of the matrix have already been transposed to account for the transpose of the [TRNPW] matrix in Eq. (7). Inspection of Eq. (11)

reveals that it can be rewritten in a more simplified matrix form just by adding a "dummy" fourth dimension to the 3-D coordinates of point p:

$$\begin{vmatrix} XWpW \\ YWpW \\ ZWpW \\ 1 \end{vmatrix} = \begin{bmatrix} TMXPW(1,1) & TMXPW(2,1) & TMXPW(3,1) & TMXPW(4,1) \\ TMXPW(1,2) & TMXPW(2,2) & TMXPW(3,2) & TMXPW(4,2) \\ TMXPW(1,3) & TMXPW(2,3) & TMXPW(3,3) & TMXPW(4,3) \\ TMXPW(1,4) & TMXPW(2,4) & TMXPW(3,4) & TMXPW(4,4) \end{bmatrix} \begin{vmatrix} XPpP \\ YPpP \\ ZPpP \\ 1 \end{vmatrix}$$

$$= [TMXPW]^T \begin{vmatrix} XPpP \\ YPpP \\ ZPpP \\ 1 \end{vmatrix} \tag{12}$$

Eq. (12) indicates that the transpose of the 4×4 matrix [TMXPW] may be used to project a Pylon axis vector directly into Wing-axis coordinates. This expression is the final form of the desired transformation. It is extremely important to note that the transpose of the augmented 4×4 matrix in Eq. (12) is not the same as the inverse of the matrix. The augmented 4×4 form of the combined rotation/translation transformation is not orthogonal (as its 3×3 rotational component is) and $[TMXWP] = [TMXPW]^{-1}$ but $[TMXPW]^{-1} \neq [TMXPW]^T$. A closed-form expression for the inverse of a 4×4 positioning matrix (which will be needed for other applications) will be developed later in this section. First, however, the beauty of the 4×4 form of the transformation for multiple levels of referencing is illustrated.

Eq. (9) was developed earlier to illustrate the complicated nested transformations that result even from only two levels of geometry referencing (Adaptor to Pylon and Pylon to Wing). When the augmented form is used, the mathematics are greatly simplified even for many levels of referencing. For example, the "cumulative" transformation for the positioning of the Missile axes relative to the Global axes would be expressed simply as:

$$[TMXMG] = [TMXMR][TMXRA][TMXAP][TMXPW][TMXWG] \tag{13}$$

and Missile-axis geometry coordinates {XMpM, YMpM, ZMpM} can now be transformed to the Global system simply by premultiplying by the transpose of [TMXMG] in a form analogous to Eq. (12). A series of sequential matrix multiplications resulting in a final cumulative matrix such as that presented in Eq. (13) is sometimes referred to as a "concatenated" transformation.

A slight digression will be made at this point to develop a closed-form expression for the inverse of a 4×4 transformation. Suppose all geometry points have been defined in a higher level axis system such as Pylon axes and one desires to transform them to the next lower system

(Adaptor axes); then the matrix [TMXPA] = [TMXAP]$^{-1}$ is needed so that its transpose can be used to project the points. Although it is possible to simply compute the inverse matrix using standard matrix inversion procedures, inspection of the 4 × 4 form reveals that a much less computationally intensive closed-form solution is available. Beginning with [TMXAP]:

$$[\mathrm{TMXAP}] = \begin{bmatrix} & [\mathrm{TRNAP}] & & \begin{matrix}0\\0\\0\end{matrix} \\ \mathrm{XPAP} & \mathrm{YPAP} & \mathrm{ZPAP} & 1 \end{bmatrix} \tag{14}$$

it is desirable to define the terms of [TMXPA] as:

$$[\mathrm{TMXPA}] = [\mathrm{TMXAP}]^{-1} = \begin{bmatrix} & [\mathrm{TRNPA}] & & \begin{matrix}0\\0\\0\end{matrix} \\ \mathrm{XAPA} & \mathrm{YAPA} & \mathrm{ZAPA} & 1 \end{bmatrix} \tag{15}$$

The 3 × 3 rotational part of [TMXPA] can be immediately defined as the transpose of the rotational part of [TMXAP] because of the orthogonality of rotations, [TRNPA] = [TRNAP]^{T}. The translational terms of [TMXPA] can then be defined according to:

$$\begin{vmatrix}\mathrm{XAPA}\\ \mathrm{YAPA}\\ \mathrm{ZAPA}\end{vmatrix} = [\mathrm{TRNAP}] \begin{vmatrix}-\mathrm{XPAP}\\ -\mathrm{YPAP}\\ -\mathrm{ZPAP}\end{vmatrix} = [\mathrm{TRNAP}] \begin{vmatrix}\mathrm{XPPA}\\ \mathrm{YPPA}\\ \mathrm{ZPPA}\end{vmatrix} \tag{16}$$

Finally, a couple of comments about modern graphics languages and mathematics are in order. All of the equations in this section have been developed in standard mathematical convention wherein vectors are represented in column form and matrix multiplication is performed by premultiplying the existing matrix or vector from the left. The matrices are represented in a "row-major" form in which matrix elements are filled in across the top row first, followed by the second and succeeding rows. Over the years, graphics capabilities at AEDC have been implemented using three different graphics languages: Apollo Graphics Meta Resource® (GMR), Programmers Hierarchal Interactive Graphics Standard® (PHIGS), and OpenGL®. (The latest version of the graphics program at AEDC, known as TVIS (Trajectory VISualization), is written in OpenGL.) Each of these languages is generally optimized for high-speed computation

and may not necessarily be compatible with standard mathematical convention. In addition, many modern graphics languages are written for compatibility with the "C++" programming language, which represents matrices in a "column-major" form. For such languages, the matrix elements are loaded in column order in the computer code, but the internal math (some of which is performed by specialized accelerated graphics routines) is performed consistently with the equations presented herein.

For reasons of computational efficiency, the OpenGL language, in particular, performs mathematical functions by a somewhat nonstandard mathematical convention. OpenGL represents vectors as rows rather than columns and performs matrix multiplication by post-multiplication from the right. In OpenGL math, Eq. (7) would be written as:

$$\begin{vmatrix} XWpW \\ YWpW \\ ZWpW \\ 1 \end{vmatrix}^{T} = \{XWpW \quad YWpW \quad ZWpW \quad 1\} = \{XPpP \quad YPpP \quad ZPpP \quad 1\}[TMXPW] \tag{17}$$

where Eq. (17) is derived from Eq. (12) by simple application of the matrix identity $(AB)^T = B^T A^T$.

One of the computational efficiencies that arises from the row-major formulation used by OpenGL is that the process of projecting point coordinates from one system to another (represented in column-major form by Eq. [12]) and the process of matrix concatenation (Eq. [13]) can be combined into a single mathematical equation, as illustrated below:

$$\begin{aligned} &\{XGpG \quad YGpG \quad ZGpG \quad 1\} \\ &= \{XMpM \quad YMpM \quad ZMpM \quad 1\}[TMXMG] \\ &= \{XMpM \quad YMpM \quad ZMpM \quad 1\}[TMXMR][TMXRA][TMXAP][TMXPW][TMXWG] \end{aligned} \tag{18}$$

This formulation produces computational speed advantages because the concatenated matrix transformation converting local geometry points to the global system can be applied to each geometry point as it is read in – eliminating any requirement to save the original coordinate values defined in the original local geometry systems (as is necessary for other graphics languages that perform the point conversions at display time). Another advantage of the row-major form is that the viewing matrix (which is described in the next section) is the last matrix to be applied to the transformed global coordinates. Since the viewing matrix is at "the top of the matrix stack" (to use OpenGL terminology), it is easily accessible for the interactive modifications required to dynamically rotate, translate, or scale the image on the graphics screen.

2.3.2 Camera Positioning and View Angles

In computer graphics, the subject aircraft is generally positioned relative to the camera (or, more exactly, the Global geometry system is positioned relative to the perspective viewpoint, and then what is "seen" from that viewpoint is projected to the computer screen). In contrast, the information provided in the F-22 flight test document (reproduced in Table 1) specifies the position of the camera relative to the aircraft and the direction of the camera line of sight (the direction in which the camera is looking) relative to the aircraft. Therefore, it will be necessary to build the camera-relative-to-aircraft transformation from the data provided and then invert it to get the aircraft-relative-to-camera information used in the graphics routines.

The F-22 camera positions are specified in Table 1 in terms of the so-called "Absolute Aircraft" axis system using aircraft Fuselage Station (STA), Buttock Line (BL), and Waterline (WL) coordinates. This same system is also the Global axis system, "G," in which the graphical aircraft geometry models are built. An intermediate axis system designated by "L" (for line-of-sight axes) is defined for the camera viewpoint and direction. The XL axis is assumed to lie in the direction of the camera line of sight. The ZL axis is defined as being in the "up" direction as seen by the camera. The vector {XGLG, YGLG, ZGLG} defines the Global absolute aircraft components of the position of the camera viewpoint relative to the Global axes and is set to the STA, BL, and WL position values specified in Table 1. The "Lens Orientation" values from Table 1 are used to define yaw-pitch sequence Euler angles (PSILG for the azimuth, or yaw angle, and THALG for the pitch, or Down angle) for the direction of each camera line of sight relative to the aircraft Global geometry axes. Zero values of PSILG and THALG denote a camera looking directly forward. Using PSILG and THALG and assuming PHILG = 0.0, the yaw-pitch sequence direction cosine matrix [TRNLG] is created (using Eq. 1.3.8 of Ref. 1). The {XGLG} vector and the [TRNLG] matrix are then used to create the 4×4 augmented transformation matrix [TMXLG]. Finally, [TMXLG] is inverted to create [TMXGL] using the closed-form matrix-inversion technique described in Eqs. (16) and (17) of the previous Section.

The intermediate camera line-of-sight axes, "L," were defined consistently with the camera information provided in Table 1. Computer graphic systems, however, typically define a Camera, "C," axis system aligned with the graphics screen with the X_C coordinate positive horizontally to the right on the computer screen and the Y_C coordinate positive vertically up on the graphics screen. The camera line-of-sight direction is, therefore, coincident with the negative Z_C axis of the graphics camera axes. Another transformation matrix, which will be designated [TMXLC], must be defined for the orientation of the line-of-sight axes relative to the graphics Camera axes. This matrix contains zero translation values and a direction cosine matrix defined by a rotation of 90 deg about the Z_C axis followed by a rotation of 90 deg about the resulting new Y axis.

Finally, the total cumulative matrix for positioning the aircraft Global geometry relative to the Camera is given by:

$$[\mathrm{TMXGC}] = [\mathrm{TMXGL}][\mathrm{TMXLC}] \tag{19}$$

Many modern computer-graphics languages (including OpenGL) maintain separate modeling, viewing, and projection matrices. The modeling matrices for placing the various geometry models into the Global axis system are described in Section 2.3.1. In an OpenGL implementation, matrix [TMXGC], specified by Eq. (19), is loaded directly into the view matrix. The last step of the graphics process is to define the projection or perspective transformation matrix which maps the 3-D coordinates as seen from the camera viewpoint to the two-dimensional (2-D) graphics screen.

Although the 4×4 projection matrix that describes the perspective projection of the 3-D graphics geometry to the 2-D graphics screen could be specified directly, most high-end graphics languages provide better performing, accelerated functions for perspective transformations. Different graphics languages specify the perspective parameters according to different definitions and sign conventions, however. For OpenGL implementations, four parameters need to be specified. These are described in the next several paragraphs.

The first parameter which must be specified for OpenGL perspective implementation is the distance from the camera to the “near” clipping plane. Any object closer to the camera than this value will not be displayed. OpenGL will return an error if this value is negative (or behind the camera). A default value of 1 in. was selected for the virtual camera implementation. A consequence of this near clipping is demonstrated at the end of this section for views from the F-22 cameras mounted on the lower wing surfaces at the wingtips. Although the surface of the wing directly in front of and above the camera lens should be within the field of view of the camera, it is clipped out in the graphics views.

The next required OpenGL perspective parameter is the distance to the far clipping plane. This value is also always positive (even though it is in the negative ZC direction because a left-handed viewing coordinate system is actually used internally in OpenGL), and it must place the far clipping plane further away from the camera than the most extreme point in the aircraft geometry. OpenGL has graphical capabilities for z-buffered hidden surface removal so that surfaces which are behind other surfaces will not be shown. The resolution of these capabilities is based on the distance between the near and far planes. If the far plane is placed too far away from the camera (near the computer equivalent of infinity, for instance), the hidden-surface removal capabilities will not function correctly, and the graphics pictures may be distorted. The TVIS code has therefore been set up by default to place the far clipping plane just beyond the most extreme point of the aircraft/store geometry.

The two remaining parameters required for perspective viewing are the graphics frame aspect ratio and field of view. OpenGL has a standard graphics function, glPerspective, which uses an aspect ratio defined as frame width/height (instead of the more conventional height/width) and a vertical field-of-view angle, FOVy, as input arguments. The aspect ratio and FOVy values for the F-22 cameras were previously described in Section 2.2. The glPerspective call creates a rectangular view which is then sized to fit the largest area possible in the display

window on the graphics screen. If the display window on the graphics screen has an aspect ratio different from the assumed rectangular film frame, blank space will be displayed at the top or right of the graphics area. Of course, as has already been noted in Fig. 1, the film frame of the 1VN camera is not rectangular. No attempts were made to model the rounded vertical borders of the film frame in the graphics program; instead, the smallest rectangular border that the 1VN frame fits within was modeled. It is possible, however, to postprocess the graphics images to better emulate the exact view from the 1VN camera. Figure 10, for example, illustrates a rectangular view from the graphics program over which a film frame border has been drawn using a 2-D graphical "paint" program.

When a real camera lens is focused on an object at a finite distance in front of the camera, there is an additional region in front of and behind the object that is also in focus. This in-focus region is called the depth of field and is a function primarily of the aperture or light-receiving area of the lens. OpenGL and other graphics languages have advanced capabilities to emulate depth of field using sophisticated fogging techniques and near and far depth-of-field planes. Such advanced capabilities are extremely computer intensive and were not warranted for the virtual camera model. In essence, the virtual model represents a "pin-hole" camera for which all objects in the field of view are in focus.

A simple test was implemented to make sure that the aircraft was correctly positioned relative to the camera viewpoint for each of the 12 F-22 camera locations. A simple cube geometry model was built (6 in. on each side) and placed in the aircraft configuration at the locations specified by the {XGLG} vectors for each camera, as shown in Fig. 11. When each camera view was called for, the expected views of the inside of surfaces of the cubes from the cube centers were obtained.

The wind tunnel ground-simulation trajectory data for different stores may be generated at different time steps. For example, in the F-22 wind tunnel trajectory testing, the time step for the external tank and missile cluster releases was 0.00125 sec; for the autopilot-off AIM-120C and the AIM-9M it was 0.0025 sec; and for the autopilot-on AIM-120C it was 0.0002 sec. Only the data at every 0.01 seconds were actually stored in the final wind tunnel data files for each store, however. A capability was added to the TVIS graphics visualization program to form an Akima spline (Ref. 3) function of the trajectory data and interpolate it to the 0.005-sec time step of the 1VN cameras. For this interpolation the yaw, pitch, and roll angles of the store were converted to Euler parameters or quaternions (Section 4.3.2 of Ref. 2), then interpolated, normalized, and converted back to yaw-pitch-roll form. This conversion was necessary because trigonometric quadrant-check errors result for tumbling stores when pitch angles near –90 deg are interpolated to values beyond –90 deg or when yaw or roll goes beyond ±180 deg. Use of quaternions avoids the need for elaborate quadrant-checking algorithms, as discussed in Ref. 2.

Most wind tunnel trajectories for the F-22 were obtained on the right side of the aircraft. The flight test aircraft, however, are being designed to release only from the left side of the aircraft,

with the right bays reserved for flight test instrumentation. The flight test cameras are, therefore, positioned to cover only left-side releases. Wind tunnel graphics views must be mirrored to the left side of the aircraft for direct comparisons with flight film. As a temporary stopgap approach, however, the cameras themselves were mirrored over to the right side of the aircraft for views of the right-side wind tunnel data. Station 4mir is, for example, the same as flight test station 4 but is mirrored to the flare bay on the right side of the aircraft for looking at right-side wind tunnel data.

Figures 12 through 14 show graphic views of separations of various classes of missiles from the F-22 that are based on data from a recent F-22 wind tunnel test. In addition to the camera perspective views, orthogonal right, bottom, and front views are provided so that some quantification of the perspective distortion of the camera data can be obtained. An interesting mental exercise for the reader might be to look at the different camera views and attempt to synthesize them into a mental picture of the overall store motion. The orthogonal views then can be used to check the accuracy of that mental understanding. Even experts in the store separation field have had difficulty in mentally combining the views from the different camera perspectives. Views were generated for all of the relevant camera orientations at each camera station. Only views from orientations selected by the author for illustrative purposes are presented in the figures.

3.0 EFFECTS OF AIRCRAFT MOTION ON CAMERA VIEWS DURING THE STORE-RELEASE EVENT

Whenever an aircraft releases a store in flight, the aircraft undergoes a transient maneuver in response to that release. As the aircraft maneuvers, it carries its cameras with it. The aircraft motion can result in false apparent motion of the released store in the camera views—motion which is actually representative of camera/aircraft motion relative to the store rather than store motion relative to the aircraft. The aircraft response to the release of a store is dependent on the aerodynamic and inertial significance of that store. For the F-22, the most significant store in that regard is the full 600-gallon tank.

The F-22 can carry up to four 600-gallon tanks, which weigh about 5000 pounds each. In some extreme scenarios it may be necessary to release all four tanks nearly simultaneously (outboard pair followed by inboard pair). At this point, however, only release of a single tank at a time is being planned for preliminary flight tests. The F-22 response to the release of a single tank has many aspects. First, as the tank is released, the aircraft lift-to-weight ratio (load factor N_N = Lift/Weight) becomes instantly unbalanced as the aircraft loses 5000 pounds of its weight. The aircraft has an instantaneous increase in vertical acceleration (often referred to as “g-jump”). More importantly, before the release, the aircraft is usually trimmed for some nonrolling, steady-state flight condition. The instant loss of the aerodynamics and weight of the tank results in large center-of-pressure and center-of-gravity shifts for the aircraft which in turn result in a transient untrimmed maneuver until trim can be reestablished. As a single tank is released from one side of the aircraft, the unbalanced left and right wing loadings also result in an immediate roll of the aircraft wing away from the store. Because the flight test cameras are “fixed mounted” in the

aircraft, the roll and other transient maneuvers will indicate an additional relative motion between the cameras and the released store (Ref. 4). None of the effects of these transient aircraft store-release maneuvers are included in the wind tunnel ground-test simulation. Tunnel trajectories assume that the store release does not affect the aircraft (an entirely valid assumption for all but large, heavy stores such as the F-22 fuel tank).

To isolate the flight trajectory motions of the store relative to inertial space or to some earth-fixed reference system, the transient maneuver motion of the aircraft system relative to inertial space must be removed from the camera-reduced motion of the store relative to the aircraft. One possible method for performing this correction post-flight is outlined here. 1) The maneuver motion of the aircraft measured in flight must be included in a regenerated postflight ground simulation using the arbitrary aircraft maneuver capability recently developed to support the F-22 roll-rate studies (Ref. 2). Graphics camera views of the recomputed maneuvering simulations should then better match the flight camera data for the heavy stores. 2) If desired, the information from the postflight simulations of step 1 can then be used to transform the film-reduced store-relative-to-aircraft flight data to a store-relative-to-inertia system.

4.0 CONCLUSIONS AND RECOMMENDATIONS

A computer graphics capability has been developed for generating views of store separations which emulate the views that are generated from aircraft-mounted flight test cameras. The views include many of the perspective distortions associated with flight film data.

1. Camera views based on wind tunnel simulations should be generated for all planned flight releases of stores from aircraft. The views should be transferred to the flight test facilities, where they can be used for a quick assessment of how well the ground simulations match flight film. Such a quick assessment may allow some flight test planning decisions to be made prior to the completion of the film data reduction at the flight test range. In addition to the “frozen-image” camera views (such as are presented as figures in this report), a complete set of computer-generated, time-correlated, animated movies should be generated using existing capabilities of the TVIS computer-graphics program.

2. Wind tunnel-based simulated camera views should be used to optimize placement of flight-test cameras for maximum coverage of the flight releases.

3. Camera views of selected wind tunnel separations should be used to validate and produce uncertainty bands for the film data reduction procedures used to extract time/space position information from flight film. F-22 flight test film data, for example, will be reduced using the Edwards Store Separation Analysis System (ESSAS) photo imaging process at Edwards AFB, CA. The ESSAS system is one of a family of photogrammetry techniques related to the Image Data Automated

Positioning System (IDAPS) and its predecessor, the Graphic Attitude Determination System (GADS), used at Eglin AFB, FL. Exercise of the photogrammetry capability on "perfect" graphic camera data can be used to demonstrate "best case" accuracy ranges on how well the trajectory positions and orientations can be extracted from actual flight film.

4. Ground simulations which include the motion of the aircraft during store release–especially the transient roll maneuver of the aircraft in response to the release of fuel tanks–should be recomputed post-flight. These simulations should be used to correct the flight film data for false apparent motion of the store which is actually attributable to the motion of the aircraft.

5. The F-22 camera positions used to demonstrate the camera models in this report were based on those published in the first draft of the F-22 store separation flight test TIS AR020. Camera positions on the actual flight test aircraft have since been continuously changing as various aspects of the F-22 aircraft design mature. Some of those changes have even been made in response to the computer visualization techniques presented herein. Although camera views updated to support the F-22 flight tests have been regenerated as each hardware change occurs, none of those updates is included in this report. The purpose of the report is to describe the computer graphics techniques themselves and not to present current F-22 separation data.

6. In the virtual camera techniques presented herein, the cameras are assumed to be rigidly mounted to a rigid airframe. Structural flexing of an aircraft wing at realistic maneuver/aerodynamic loading situations, however, may cause the wingtip (and any associated tip camera stations) to deflect vertically relative to the aircraft center body during flight. The wing may also bend in flight, changing the camera line-of-sight direction of the wingtip-mounted cameras. No capability to distort the geometry of the aircraft or to move the camera positions to simulate structural flexing is included in the current virtual camera model. If, however, separate structural flexing simulations should be available so that the flexed camera positions and line-of-sight directions could be provided, the wingtip camera view could be easily regenerated from an updated viewing position (although nondistorted wingtip geometry would still be used in the graphics views).

REFERENCES

1. Keen, K. S., Clippard, R. L., and Thomson, W. G. "Enhancements of Computer Graphic Systems for the Qualitative Evaluation of Store Separation Trajectories." Paper presented at the 8th Aircraft/Stores Compatibility Symposium, Ft. Walton Beach, FL, October 23-25, 1990.

2. Keen, K. S. "Equations for Store Separation Motion Simulations and Instrumented Model Data Reduction." AEDC-TR-95-12 (AD-A3133960, August 1996.

3. Akima, Hiroshi. "A New Method of Interpolation and Smooth Curve Fitting Based on Local Procedures." *Journal of the Association for Computing Machinery*, Vol. 17, No. 4, October 1970, pp. 589-602.

4. Gersch, E. "A New Store Separation Data Reduction Technique." Proceedings of the 7th Aircraft/Stores Compatibility Symposium, Wright-Patterson AFB, OH, April 1986.

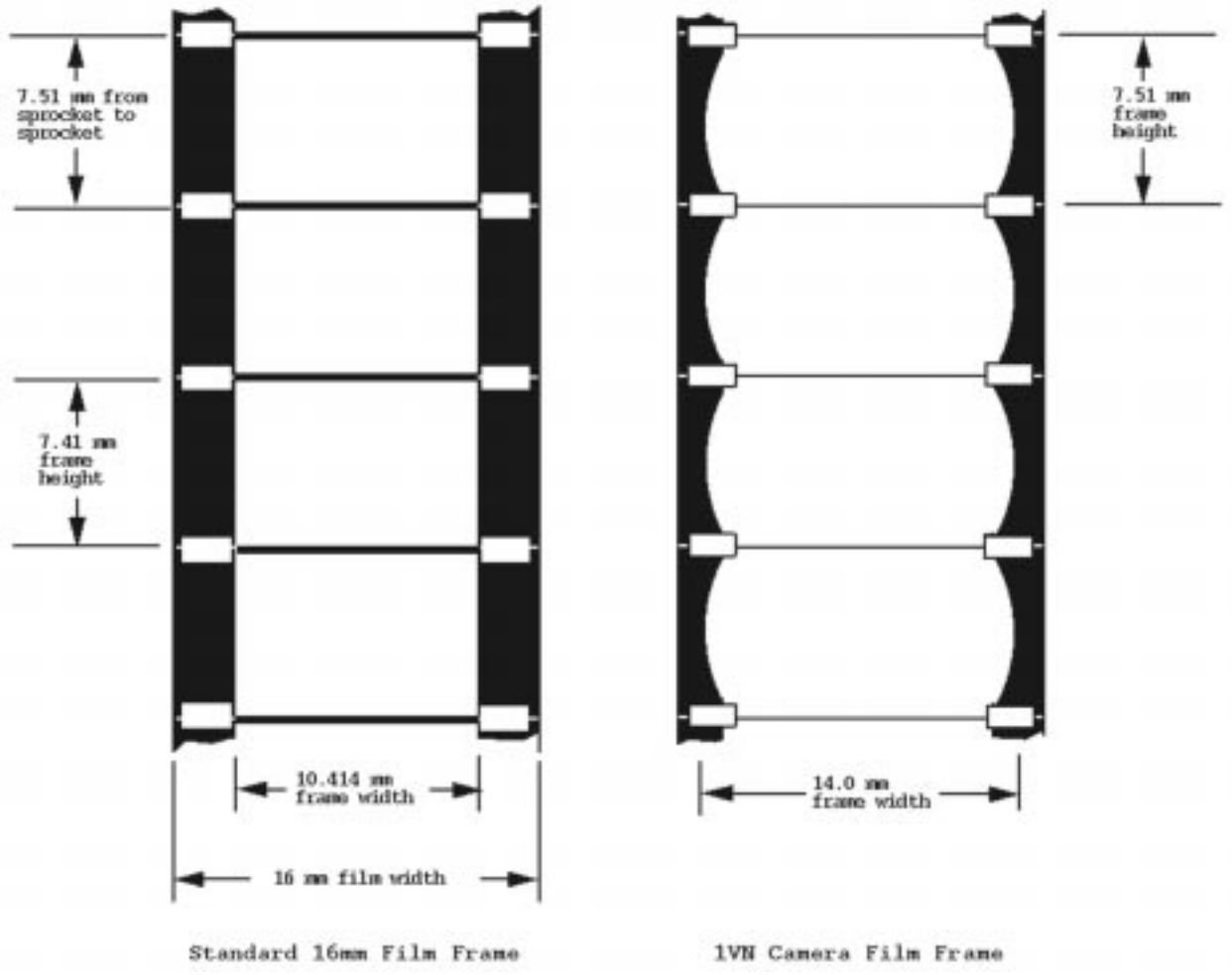

Figure 1. 16-mm film frame for the 1VN camera.

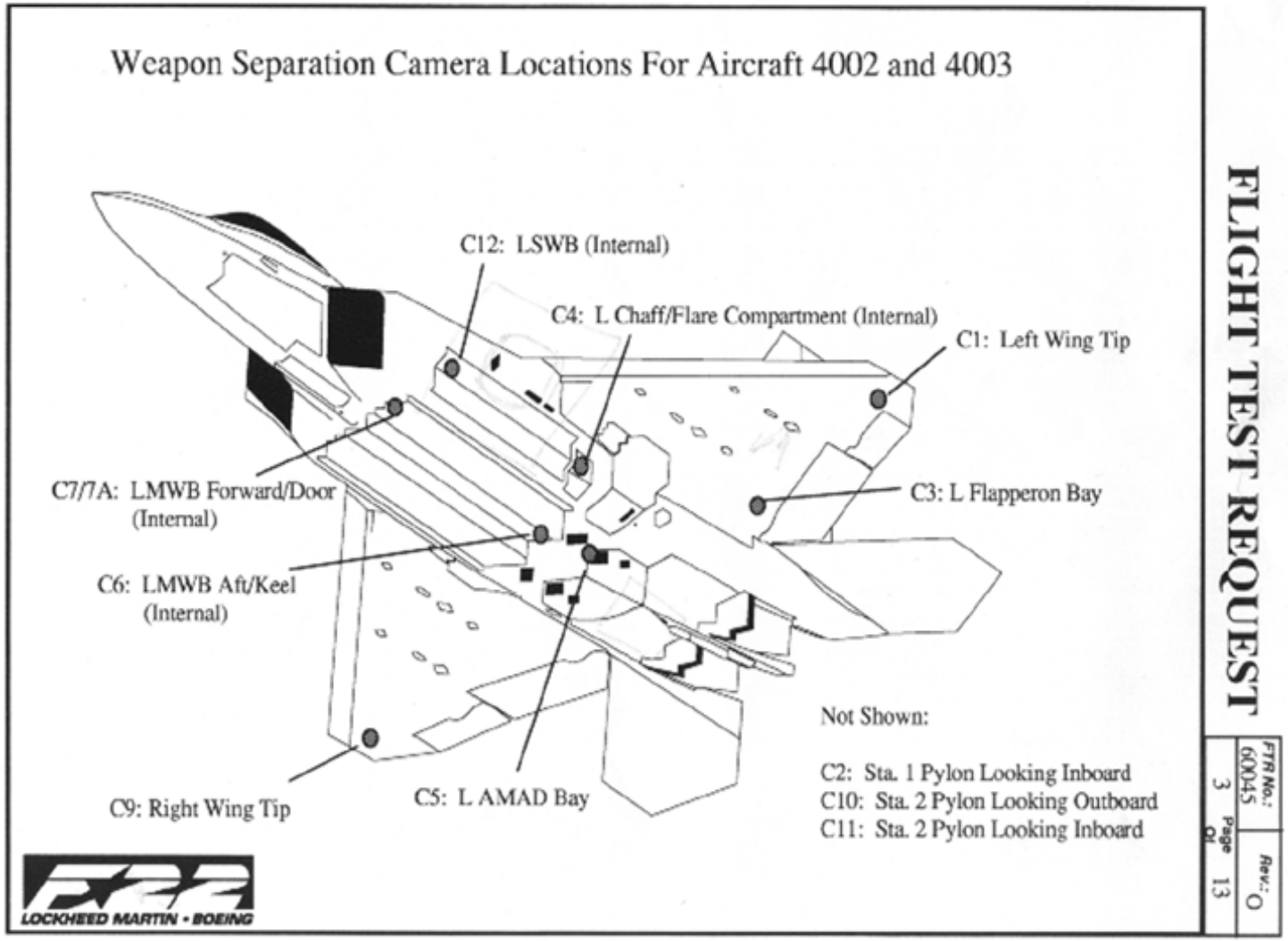

Figure 2. F22 camera locations.

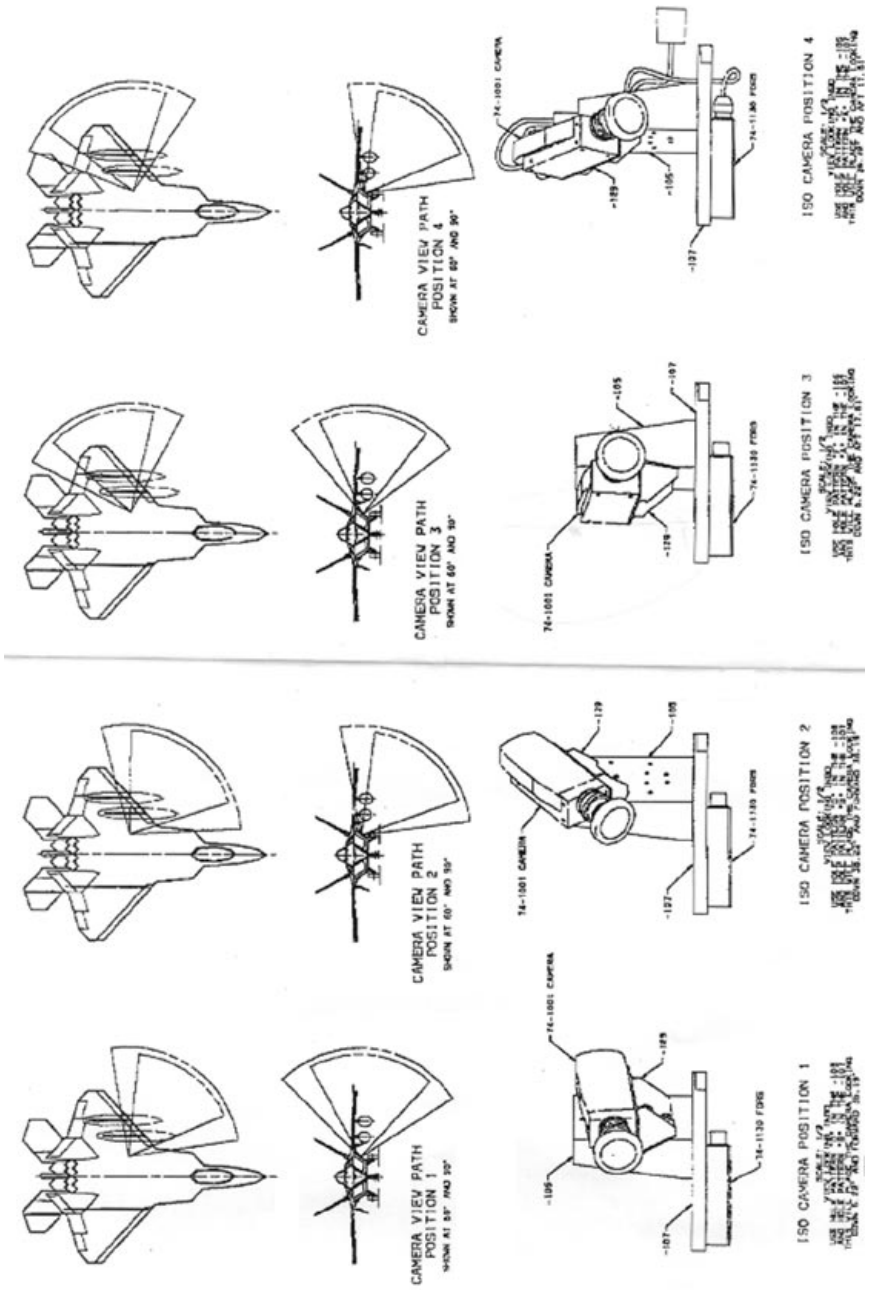

Figure 3. Support brackets for cameras at Station 4.

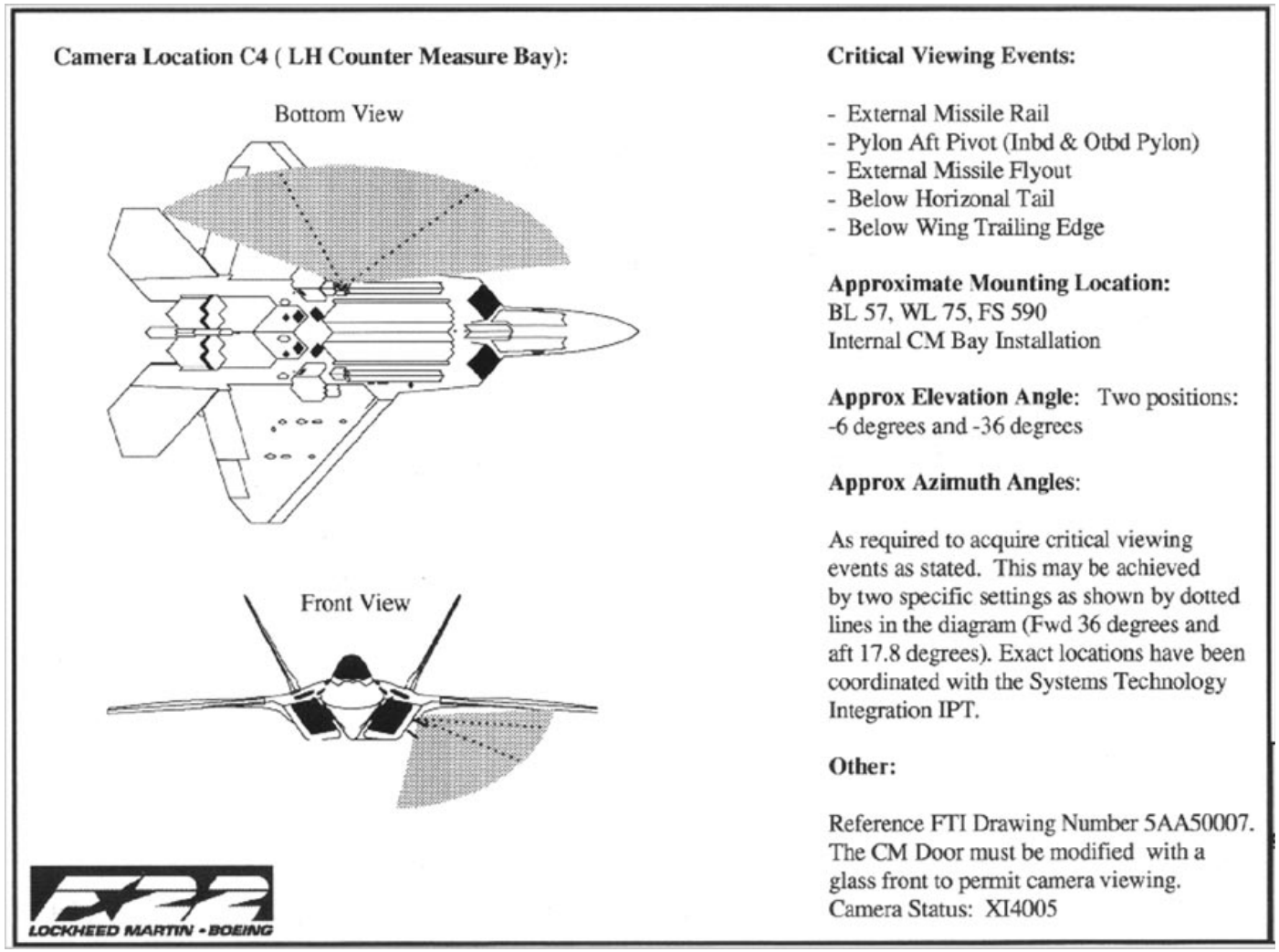

Figure 4. Line-of-sight directions for different camera mountings at Station 4.

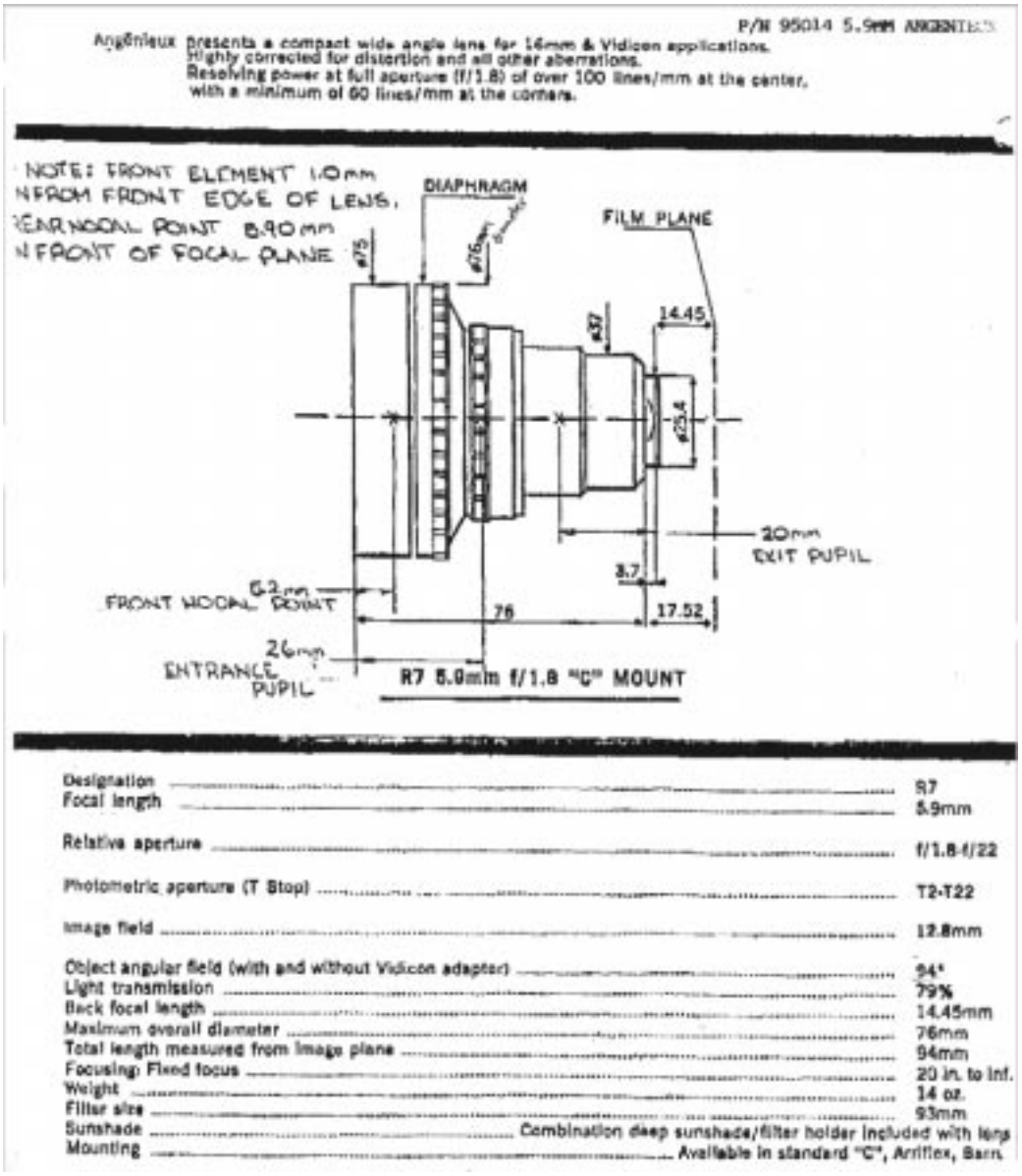

Figure 5. Augenieux R7 lens specifications.

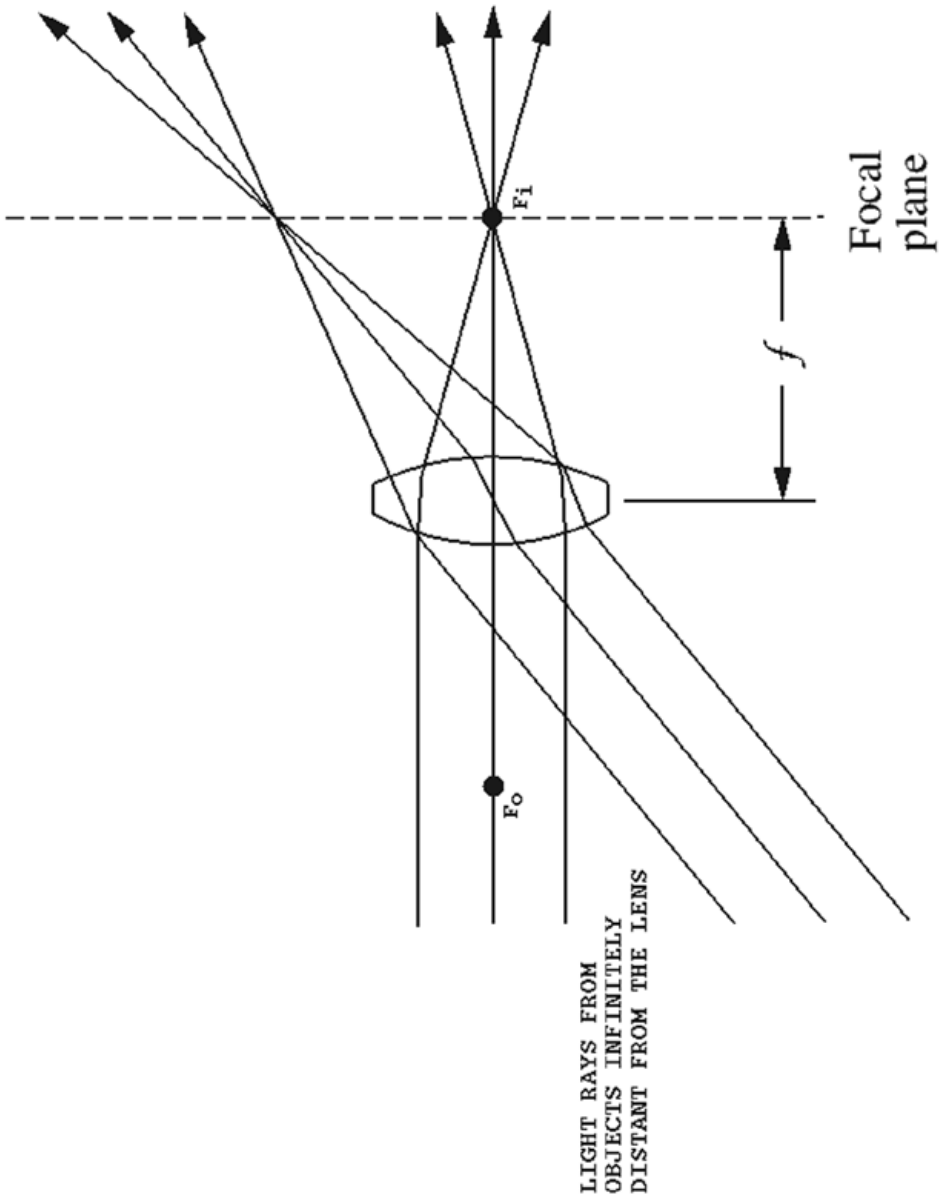

Figure 6. Focal length of a simple thin lens.

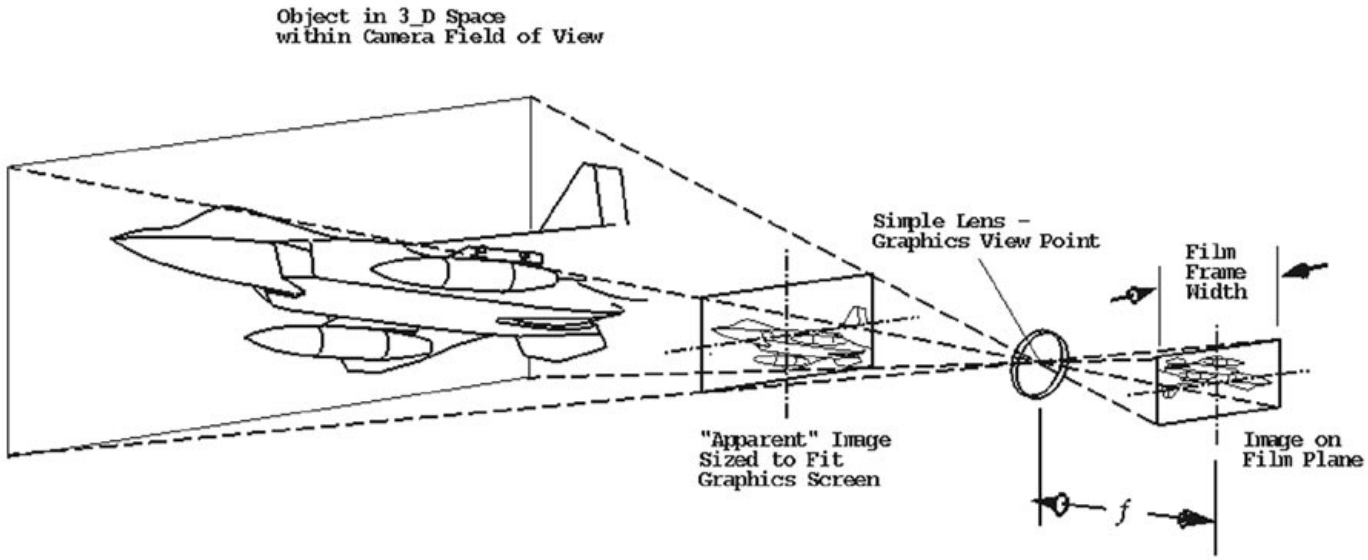

Figure 7. Field of view for a simple thin-lens camera focused at infinity.

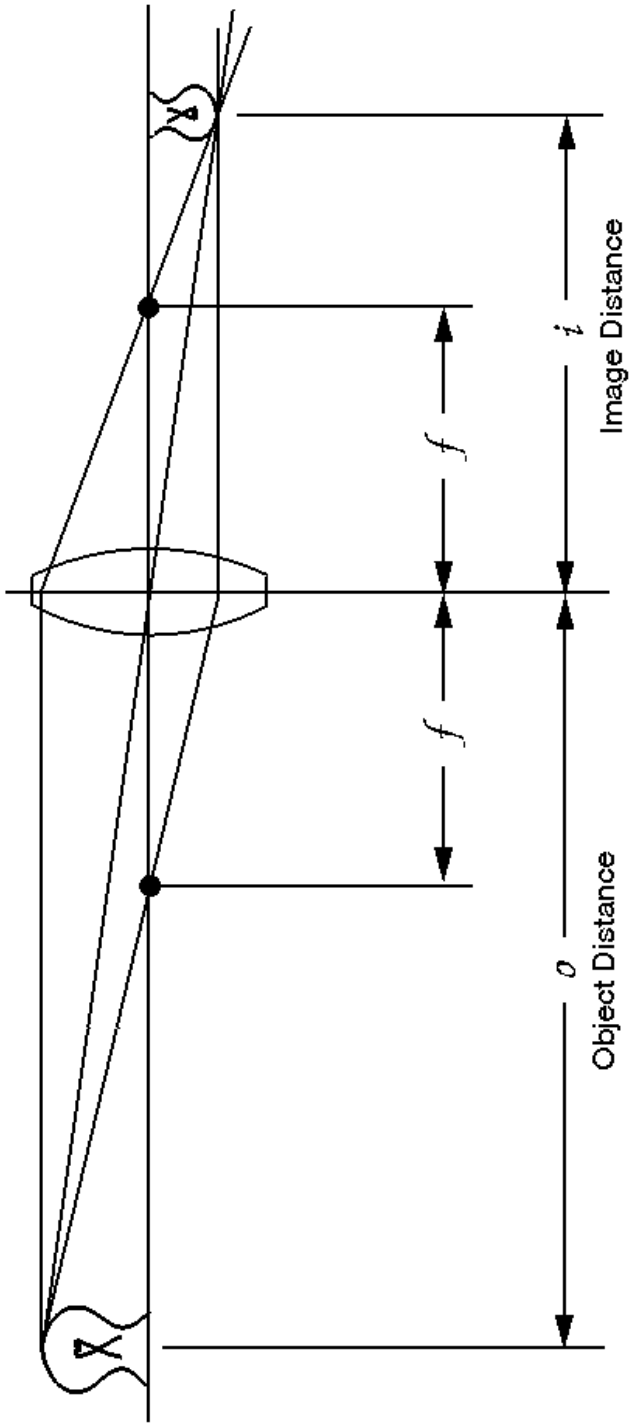

Figure 8. A simple thin lens focused on an object at a finite distance.

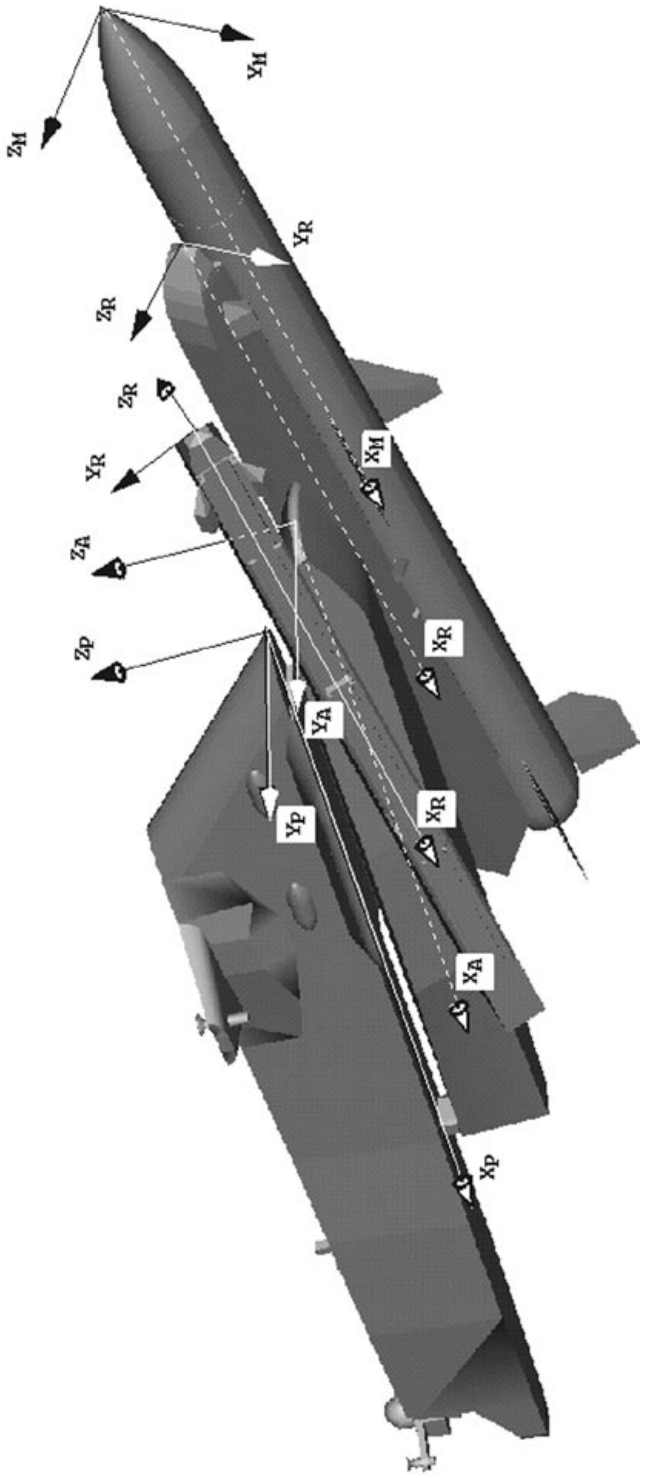

Figure 9. Local geometry axis systems for graphics models.

Figure 10. Emulation of nonrectangular 1VN frame.

Figure 11. Graphical confirmation of camera positioning.

view from 10.0-mm camera 1bmir

a. View from camera 1bmir

Figure 12. Views for an AIM-9M launch from the side bay.

view from 10.0-mm camera 3amir

b. View from camera 3amir

Figure 12. Continued.

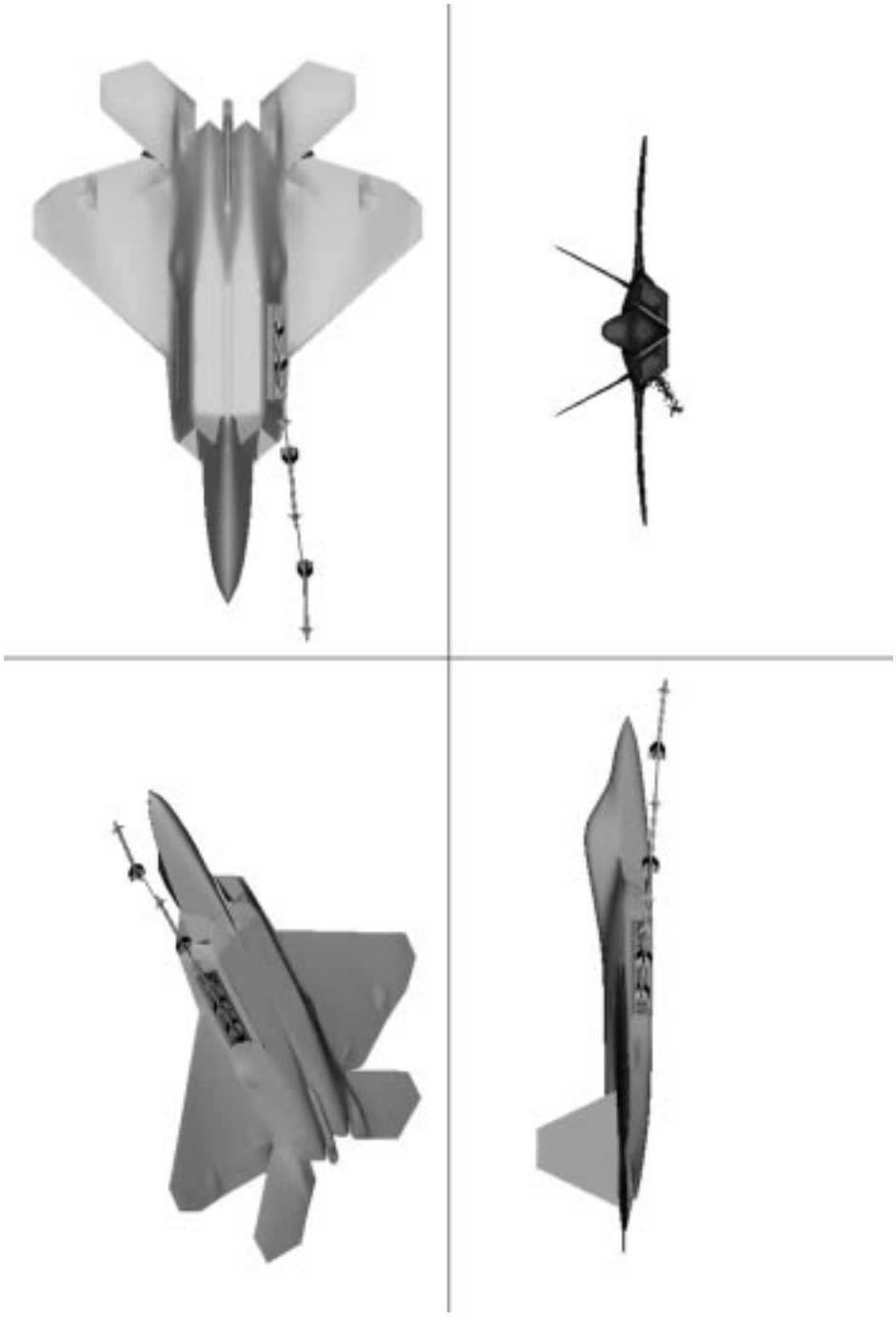

c. Orthogonal views

Figure 12. Concluded.

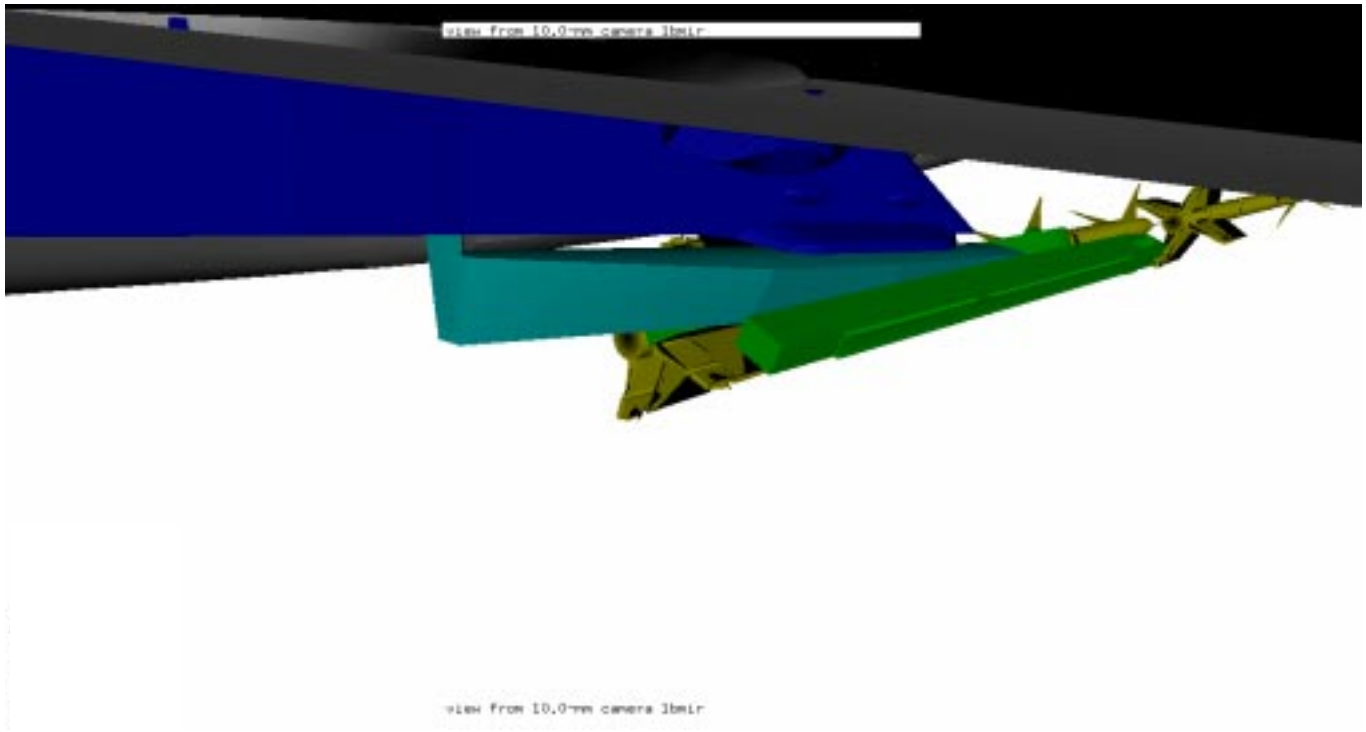

a. View from camera 1bmir

Figure 13. Views for an AIM-9m launch from the inboard wing station.

b. View from camera 3amir
Figure 13. Continued.

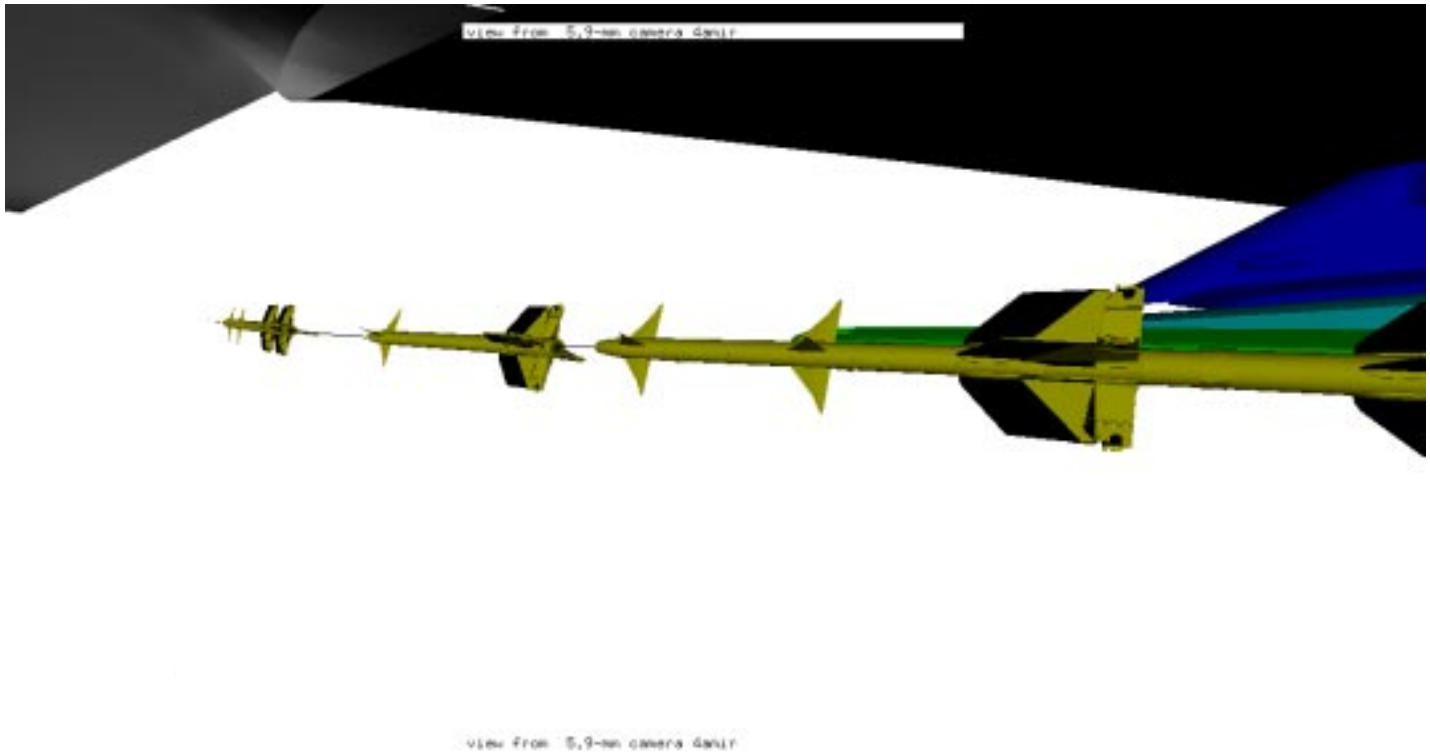

c. view from camera 4amir

Figure 13. Continued.

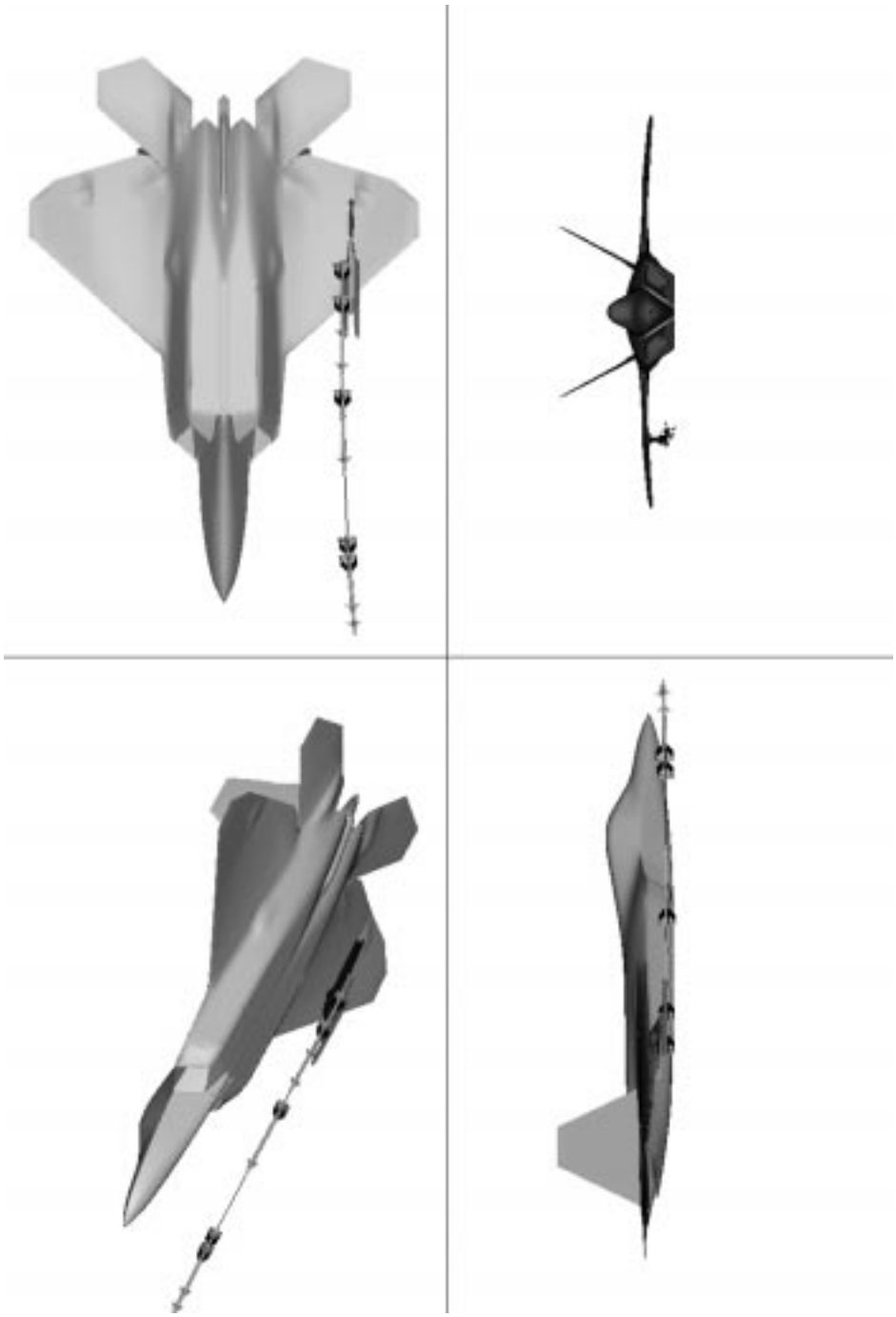

d. Orthogonal views
Figure 13. Concluded.

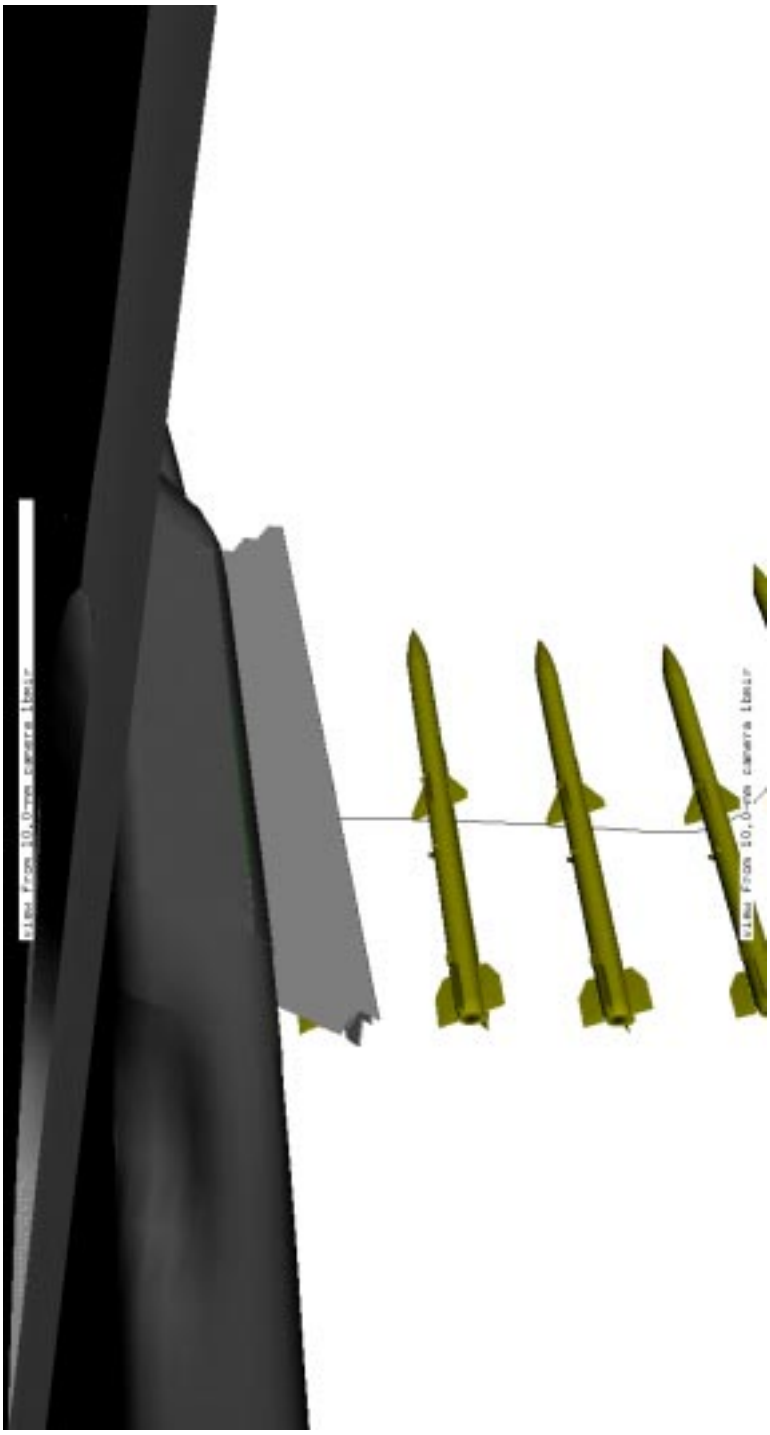

a. View from camera 1bmir

Figure 14. Views for an AIM-120C launch from the main bay.

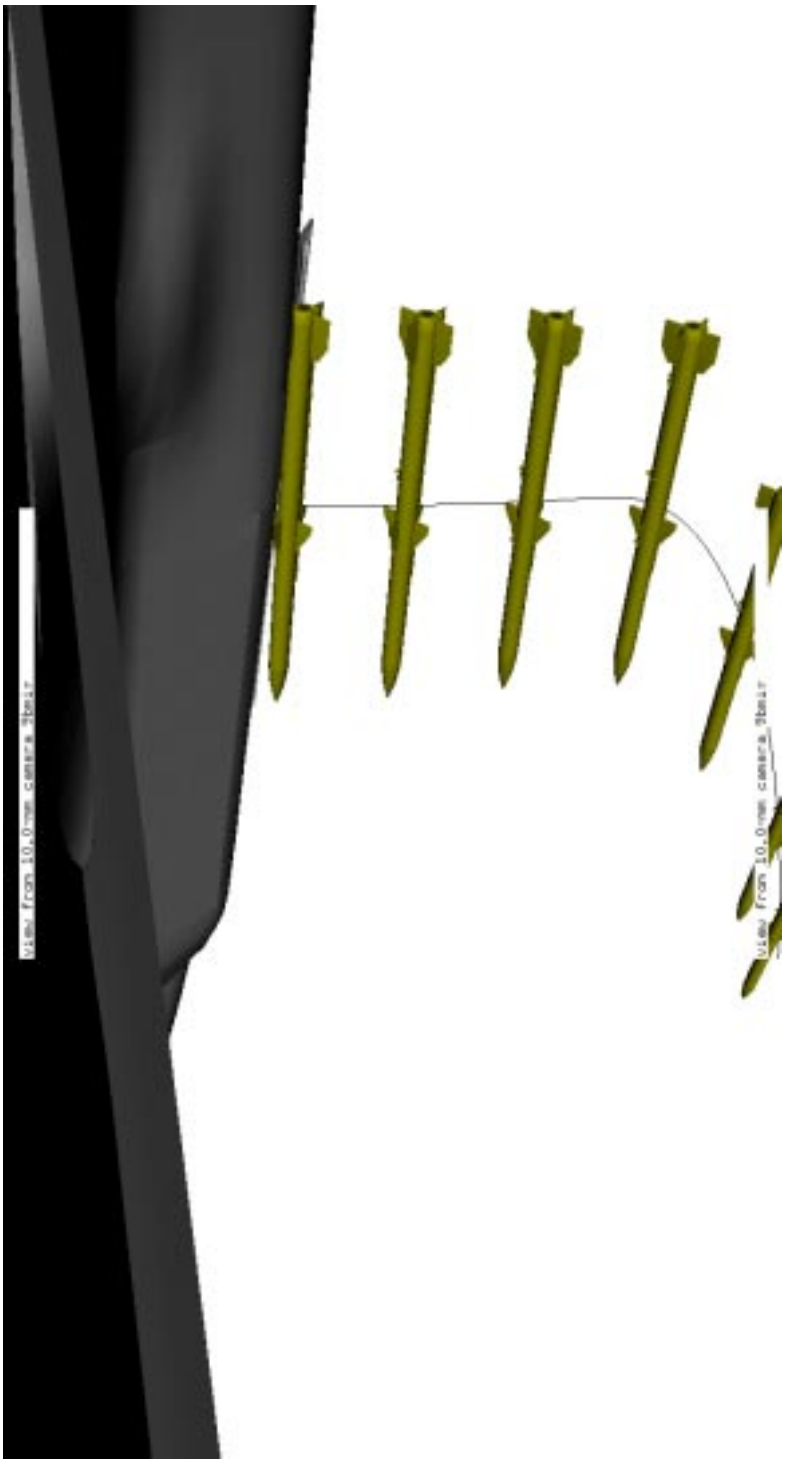

b. View from camera 9bmir
Figure 14. Continued.

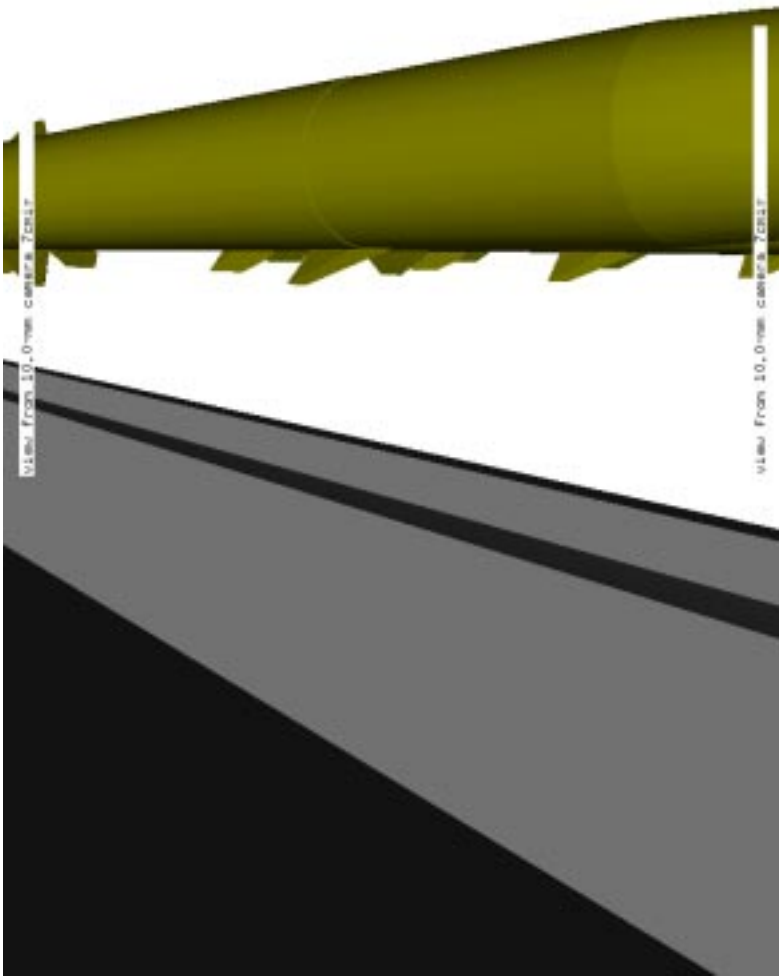

c. View from camera 7cmir
Figure 14. Continued.

d. View from camera 5dmir

Figure 14. Continued.

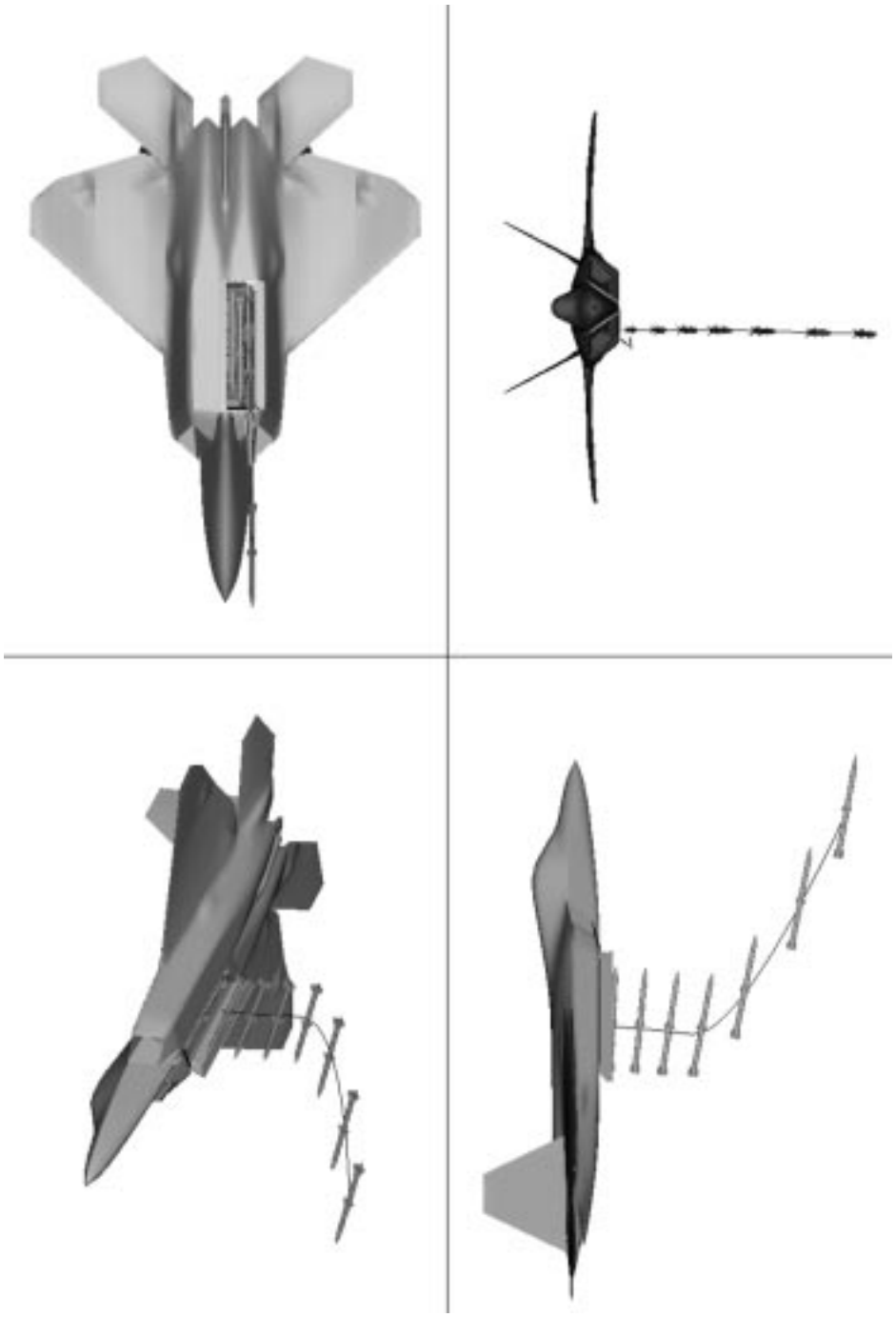

e. Orthogonal views
Figure 14. Concluded.

Table 1. F22 Camera Positions

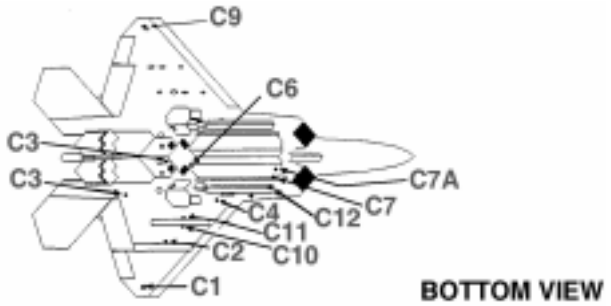

Position No.	Description	Location			Lens Orientation	Lens, mm	FOV
		FS	BL	WL			
C-1	Left Wing Tip	708	242	94	a) 15° DN, 15° INBD b) 15° DN, 45° INBD c) 15° DN, 90° INBD d) 15° DN, 135° AFT	10	41 × 55
C-2	Sta #1 Wpn Pylon-nbd	Pylon	174	Pylon	a) 10° DN, 100° INBD	10	41 × 55
C-3	Left Wing Joint (Side Body)	726	103	93	a) 15° DN, 15° OTBD b) 15° DN, 45° OTBD c) 15° DN, 90° OTBD d) 15° DN, 135° AFT	10	41 × 55
C-4	LH CM Bay Internal	590	57	75	a) 6° DN, 36° FWD b) 36° DN, 36° FWD c) 6° DN, 18° AFT d) 36° DN, 18° AFT	5.9	70 × 90
C-5	LH AMAD Bay External	620	9	53	0° -30° DN, ±120°	5.9	70 × 90
C-6	LH MWB Internal–Sta #6	569 580	5 5	76 73	a) 0° DN, 0° AZ b) 15° DN, 0° AZ c) 90° DN, 0° AZ d) 105° DN, 0° AZ e) 120° DN, 0° AZ	5.9 10	70 × 90 41 × 55
C-7	LH MWB Internal–Sta #4	451	34	66	a) 0° DN, 180° AZ b) 20° DN, 180° AZ c) 40° DN, 180° AZ	10	41 × 55
C-7A	LH MWB Internal–Sta #5	451	25	67	a) 0° DN, 180° AZ b) 20° DN, 180° AZ c) 40° DN, 180° AZ	10	41 × 55
C-9	Right Wing Tip–Lower	708	242	94	a) 15° DN, 15° INBD b) 15° DN, 45° INBD c) 15° DN, 90° INBD d) 15° DN, 135° AFT	10	41 × 55
C-10	Sta #2 Wpn Pylon–Otbd	Pylon	126	Pylon	a) 20° DN, 90° OTBD b) 20° DN, 150° AFT c) 20° DN, 45° FWD	10	41 × 55
C-11	Sta #2 Wpn Pylon–Inbd	Pylon	126	Pylon	a) 40° DN, 90° INBD b) 20° DN, 45° FWD	10	41 × 55
C-12	LH SWB–Internal	464 455	66 65.7	85 85.4	a) 30° DN, 90° OTBD b) 42° DN, 90° OTBD c) 30° DN, 90° OTBD	10	41 × 55